THE EFFECTS OF THE MATERIAL DENSITY AND DIMENSIONS OF THE LANDSLIDE ON THE GENERATED TSUNAMIS

A THESIS SUBMITTED TO
THE GRADUATE SCHOOL OF NATURAL AND APPLIED SCIENCES
OF
MIDDLE EAST TECHNICAL UNIVERSITY

BY

IŞIL İNSEL

IN PARTIAL FULLFILLMENT OF THE REQUIREMENTS
FOR
THE DEGREE OF MASTER OF SCIENCE
IN
CIVIL ENGINEERING

SEPTEMBER 2009

Approval of the thesis:

THE EFFECTS OF THE MATERIAL DENSITY AND DIMENSIONS OF THE LANDSLIDE ON THE GENERATED TSUNAMIS

submitted by **IŞIL İNSEL** in partial fulfillment of the requirements for the degree of **Master of Science in Civil Engineering Department, Middle East Technical University** by,

Prof. Dr. Canan Özgen _____
Dean, Graduate School of **Natural and Applied Sciences**

Prof. Dr. Güney Özcebe _____
Head of Department, **Civil Engineering**

Prof. Dr. Ahmet Cevdet Yalçıner _____
Supervisor, **Civil Engineering Dept., METU**

Examining Committee Members:

Prof. Dr. Ayşen Ergin _____
Civil Engineering Dept., METU

Prof. Dr. Ahmet Cevdet Yalçıner _____
Civil Engineering Dept., METU

Dr. Işıkhan Güler _____
Civil Engineering Dept., METU

Dr. Bergüzar Öztunalı Özbahçeci _____
DLH General Directorate

Civil Eng. (MSc.) Engin Bilyay _____
DLH General Directorate

Date: *07.09.2009*

I hereby declare that all information in this document has been obtained and presented in accordance with academic rules and ethical conduct. I also declare that, as required by these rules and conduct, I have fully cited and referenced all material and results that are not original to this work.

Name, Last name : Işıl İnsel

Signature :

ABSTRACT

THE EFFECTS OF THE MATERIAL DENSITY AND DIMENSIONS OF THE LANDSLIDE ON THE GENERATED TSUNAMIS

İnsel, Işıl

M.Sc., Department of Civil Engineering

Supervisor: Prof. Dr. Ahmet Cevdet Yalçıner

September 2009, 70 pages

In this thesis study; mechanism and modeling of tsunamis generated by landslides are investigated. Landslide parameters affecting the surface wave characterisics are studied. In order to understand occurance of this kind of tsunamis, among many historical tsunamis, the ones that are triggered by landslides are detected and studied. The generation of the landslide generated tsunamis are modeled using TWO-LAYER model, which solves nonlinear long wave equations simultaneously within two interfacing layers with necessary boundary conditions at the sea bed, interface and water surface. The model is applied to one of the possible landslides at offshore Yalova in the Sea of Marmara. Two of the controlling parameters, which are the density and the thickness of the slid material, are analysed and a sensitivity analysis is performed to determine the level of their effects on the evolution and amplitude of the tsunami source. Furthermore, the propagation and coastal amplification of the landslide generated waves are investigated using the tsunami simulation and visualization code NAMI DANCE. The results are presented, compared and discussed.

Keywords: Tsunami, submarine landslides, tsunami modeling, tsunami simulation, Sea of Marmara, tsunami generation

ÖZ

HEYELAN MALZEMESİNİN YOĞUNLUĞU VE BOYUTLARININ TSUNAMİ OLUŞUM VE HAREKETİNE ETKİSİ

İnsel, Işıl

Yüksek Lisans, İnşaat Mühendisliği Bölümü

Tez Yöneticisi: Prof. Dr. Ahmet Cevdet Yalçıner

Eylül 2009, 70 sayfa

Bu tezde, heyelan etkisi ile oluşan depreşim dalgalarının (tsunamilerin) mekanizması ve modellemesi çalışılmıştır. Yüzey dalga karakteristiklerini etkileyen heyelan parametreleri araştırılmıştır. Heyelan etkisi ile oluşan tsunamileri anlamak için bir çok tarihsel tsunami arasından heyelan etkisi ile oluşanlar saptanmış ve genel özellikleri verilmiştir. Heyelan etkisi ile oluşan tsunamilerin benzetimi TWO-LAYER modeli ile yapılmıştır. Bu model, doğrusal olmayan uzun dalga denklemlerini, iki arayüz içerisinde, deniz tabanındaki, arayüzdeki ve su yüzeyindeki gerekli sınır koşulları ile çözer. Model, Marmara Denizi'ndeki olası heyelanlardan biri olan Yalova açıkları heyelanına uygulanmıştır. Kontrol parametrelerinden ikisi olan kayan malzemenin yoğunluğu ve kalınlığı analiz edilmiş ve tsunami kaynağının oluşmasında ve büyüklüğündeki etki düzeyini belirlemek amacı ile duyarlılık analizi yapılmıştır. Buna ek olarak, heyelan etkisi ile oluşan dalgaların ilerlemesi ve kıyıdaki yükselmesi tsunami benzetim ve canlandırma kodu olan NAMI DANCE ile incelenmiştir. Sonuçlar karşılaştırmalı olarak sunulmuş ve tartışılmıştır.

Anahtar Kelimeler: Tsunami, heyelan, modelleme, benzetim, Marmara Denizi

ACKNOWLEDGEMENTS

The author wishes to express her deepest gratitude to her supervisor Prof. Dr. Ahmet Cevdet Yalçıner not only for his guidance throughout the thesis but also giving the author research opportunities, his encouragement during working and being incredible during travel times. The author also would like to thank Prof. Dr. Ayşen Ergin for her contributions to author's coastal engineering education, her encouragement and being a role model as an intructor and as a person. The author would like to thank Dr. Işıkhan Güler for sharing his valuable knowledge and experience throughout the author's education.

The author also would like to thank all Ocean Engineering Research Center staff for being the best collegues, warm and friendly atmosphere and being as close as a family. The author appreciates the guidance and friendship of Ms. Ceren Özer, Ms. Hülya Karakuş, Mr. Cüneyt Baykal, Mr. Mustafa Esen and Ms. Gülizar Özyurt, and especially Ms. Derya Itır Dilmen and Ms. Ayşe Karancı for being amazing roommates.

Drs. Andrey Zaytsev and Anton Chernov are kindly acknowledged for their efforts and success on development of the simulation and visualization code NAMI DANCE.

At last but definitely not least, the author would like to thank her family members for supporting the author with endless love, patience and encouragement.

This study is partly supported by Europern Union Project TRANSFER (Tsunami Risk and Strategies for the European Region) and Istanbul Metropolitan Municipality project "Simulation And Vulnerability Analysis Of Tsunamis Affecting The Istanbul Coasts".

To my family

TABLE OF CONTENTS

LIST OF FIGURES

LIST OF TABLES

LIST OF SYMBOLS

c_0 : linear long wave speed

u_s: speed of slide

a_s: acceleration of slide

d: depth of water above the slide

V: volume of the slide

B_t: thickness of the slide

m: slope of the landslide location

s: slide distance

t: time

Fr: Froude Number

h: still water depth

η: water surface elevation

M, N: Water discharge

IF, JF: Dimensions in x and y directions

g: gravitational acceleration

t_{end}: duration of simulation

ρ: density of the fluid

α: ρ_1/ρ_2 (subscripts 1 and 2 symbolize the upper and lower layers respectively)

β: h_1/h_2 (subscripts 1 and 2 symbolize the upper and lower layers respectively)

CHAPTER 1

INTRODUCTION

Tsunamis can be considered as one of the most important marine hazards. A tsunami is a series of ocean waves of extremely long wave length (and/or long period) generated in a body of water by an impulsive disturbance that displaces the water (Yalciner et. al., 2005). Tsunamis are different from wind waves so they have different propagation characteristics and shoreline consequences. Periods, wavelengths and velocities of tsunamis are so much larger than wind-driven waves.

A tsunami can have a period in the range of ten minutes to two hours and a wavelength in excess of 500 km. It is because of their long wavelengths that tsunamis behave as shallow-water waves. The rate at which a wave loses its energy is inversely related to its wavelength. Since a tsunami has a very large wave length, it will lose little energy as it propagates. Hence in very deep water, a tsunami will travel at high speeds and travel great transoceanic distances with limited energy loss. As an example, an unnoticed tsunami can travel about 890 km/hr in the ocean on the depth about 6000m, as the equivalent speed of a jet plane. This means, tsunami waves can cross oceans in hours.

Although tsunamis are generally triggered by earthquakes, they are often generated by other natural events such as submarine landslides, volcanic eruptions or meteorites.

Recent evidence collected during marine surveys implies that submarine mass movements or failures such as underwater landslides, slumps or subsidence events are also responsible for the generation of tsunamis. These important mechanisms

shape and move vast quantities of sediment down the continental slopes. The underwater failures as well as collapses of volcanic edifices, which are generally triggered by earthquakes, leave a void behind and disturb the overlying water column. The rapid movement of the water body at the failure area generates tsunami waves which evolve and start propagation rapidly. Since underwater failures on the continental slopes are near shore, the generated waves arrive to the target shoreline in a short time with a low dispersion and cause extreme run-up (Yalciner et al., 2002).

Mechanism of landslide generated tsunamis are rather difficult comparing to the tsunamis of seismic origin. In this thesis study; mechanism and modeling of tsunamis generated by landslides are investigated. Landslide parameters affecting the amplitude of the tsunami source, the characterisics of initial wave, the related historical events, the propagation of the landslide generated tsunamis are studied using specifically written codes TWO LAYER and NAMI DANCE. The models are applied to one of the possible landslides at offshore Yalova in the Sea of Marmara. Two of the controlling parameters, which are the density and the thickness of the slid material, are analysed and a sensitivity analysis is performed to determine the level of their effects on the evolution and amplitude of the tsunami source. Furthermore, the propagation and coastal amplification of the landslide generated waves in the sea of Maramara are investigated. The results are presented, compared and discussed.

This study consists of 7 chapters. In Chapter 1 an introduction and brief information is given about landslide generated tsunamis. Literature survey is given in Chapter 2. It gives details of different approaches to landslide tsunamis such as numerical, analytical, and experimental or case studies. In Chapter 3, landslide triggered tsunami generation mechanism is given in detail including historical events and factors affecting the generation mechanism. Modeling of tsunamis generated by submarine landslides is given in Chapter 4. The theoretical and numerical backgrounds are given. Details of the numerical model TWO LAYER which solves nonlinear long wave equations simultaneously within two interfacing layers with necessary boundary conditions at the sea bed, interface and water surface.used in this study are explained in this chapter. Chapter 5 gives general characteristics, modeling, and effect of density and thickness of slid material of underwater

landslides in the Sea of Marmara at offshore Yalova case. In Chapter 6, propagation and coastal effects of the selected landslide generated tsunami case study at offshore Yalova are investigated using the tsunami simulation and visualization code NAMI DANCE. In Chapter 7, conclusion is given and the results are discussed.

CHAPTER 2

LITERATURE SURVEY

Although earthquakes are the main tsunami sources, there are some other mechanisms that may trigger tsunamis. These are mainly landslides, volcanic eruptions and meteor impacts. Tsunamis can also generate from the combination of these mechanisms as well. Landslides which may trigger tsunamis can be divided into two according to the location they occur; submarine and subaerial slides. Also landslides may split into two according to the type of sliding material as rock and mud slides. In this thesis, submarine mud slide generated tsunamis are studied. Numerical, analytical and experimental studies have been performed about landslide generated tsunamis. The followings are the recognizable studies about landslide generated tsunamis in literature.

Pelinovsky and Poplavsky (1996) define a landslide motion as: A body of definite geometric shape and assigned density is at rest on an inclined seabed. At the time t_0 the force of adhesion between the body and the inclined bed goes to zero and the body starts to move under the action of gravity. After a finite period of time the body reaches the lowest level of the inclined seabed and stops. Pelinovsky, Poplavsky (1996) proposed a simple hydrodynamic model to describe the water displacement above a moving slide. The model is based on linear potential theory for an inviscid fluid and the maximal displacement of sea water for large values of the Froude number and an analytical formula for the wave height is obtained. The maximal height of the tsunami wave depends only on the geometry of the landslide body and the basin depth. They observed that the estimates of tsunami waves generated by the Storegga Slides (Norway) are in good agreement with results of numerical simulations.

Pelinovsky and Poplavsky (1996) came up with the formula in the important case L>>d,

$$\eta_{\max} = \frac{\pi B_t^{\,2}}{4d}$$

"L" is the length of the landslide along wave direction, d is the water depth and "B_t" is the thickness of the sediment (landslide material) and "$\eta_{\max}$" is the maximum displacement of the water surface.

It follows from this study that the wave generation caused by a submarine landslide primarily depends on the volume and weight of the landslide material, its depth of deposition, the slope angle of the sliding surface, and the speed of the landslide movement.

Özbay (2000), in her thesis titled "Two-Layer Numerical Model for Tsunami Generation and Propagation" , tested TWO-LAYER model (Prepared in Tohoku University Disaster Control Research Centre in Japan by Prof. Imamura), improved it by using a regular shaped basin and performed the sensitivity analysis for the effecting parameters. By using the model TWO-LAYER, the aim is to find out the possible effects of different parameters such as water depth at the point of occurrence of tsunami generation mechanism, the geometry of the mass failure area, the slope of the sea bottom and the characteristics of the sea water such as the density etc. The model is tested numerous times in order to find out relative effects of different parameters on the obtained maximum water surface elevation histories at the selected stations as a function of time. As a case study, Özbay (2000) applied the model to the occurrence of landslide or the combination of the occurrences of the landslide(s) and fault breaks in the Sea of Marmara. The computation domain of the Sea of Marmara for the application was chosen as bounded by the longitudes 26.55°E - 29.96°E and latitudes 40.2977°N – 41.1066°N. The grid size of the domain was taken as 300m. Three different scenarios have been applied for hypothetical case studies. They are the occurrence of a landslide at the south of Yenikapı coasts, at the south of Marmara Ereğlisi coasts of İstanbul and occurrence of an earthquake at Armutlu fault and two accompanying landslides along this fault.

Alpar et. al. (2001) defined the probable underwater failures and modeling of tsunami propagation in the Sea of Marmara. According to Yalciner et. al. (2002), more than 30 tsunami events have impacted the coasts of the Sea of Marmara in the past two millenniums. These events affected İzmit Bay, the shores of İstanbul, Gemlik Bay, the shores of the Kapıdağ and Gelibolu Peninsulas throughout history. After İzmit tsunami of 17 August, 1999, available field survey run-up data and marine surveys have been conducted. Determining the slope failure potential as a possible tsunamigenic source in the Sea of Marmara was the main purpose of this study. Multibeam bathymetry, shallow and deep seismic reflection data are used. The generation, propagation and coastal amplifications of tsunamis related to earthquake and slope failure scenarios were tested by using tsunami simulation model TWO_LAYER. The maximum water surface elevations near the shores along the north and south coasts are obtained according to the selected scenarios of tsunami generation.

Okal and Synolakis (2003), motivated by the investigations of the catastrophic tsunami of 1998 in Papua New Guinea, use physical models to evaluate and compare the orders of magnitude of the energy generated into a tsunami wave by seismic dislocations and underwater slumps. Writers conclude that the total energy generated by the two sources can be comparable. However, the slumping source results in a low-frequency deficiency in the far field because it is shown to be fundamentally dipolar in nature.

Fine et al. (2003) compared submarine and subaerial slides as well as rigid body and viscous slides in their study. They indicated that numerical modeling of tsunamis caused by submarine slides and slumps is a much more complicated problem than simulation of seismically-generated tsunamis. The durations of the slide deformation and propagation are sufficiently long that they affect the characteristics of the surface waves. As a consequence, coupling between the slide body and the surface waves must be considered. Moreover, the landslide shape changes significantly during slide movement, causing the slide to modify the surface waves it has generated. Fine, et. al. (2003) concluded that a rigid body slide has greater tsunami- generating efficiency and produces much higher tsunami waves than a viscous slide. However,

the viscous slide model is the model of choice as it is more realistic for engineering design. They also concluded that the maximum wave height and energy of generated surface waves depend on various slide parameters including: slide volume, type of slide (viscous or rigid), slide density, slide position (relative height or depth), and slope angle. Also, the critical parameter determining the generation of surface waves is the Froude number (the ratio between the slide and wave speeds).

Murty (2003) studied tsunami wave height dependence on landslide volume. Based on an incomplete data set of volume V of slide versus maximum amplitude H of the resulting tsunami waves, gleaned through available literature, a simple linear regression relationship was developed. Another partial data set was developed also from published literature, on V versus H values, based on numerical models. It was found that the agreement between the results of the numerical simulations and the observations is rather poor. Murty, in his paper, states there are other parameters which also play important roles. These are; a) depth of the slide, b) angle of the slide, c) total distance moved by the slide, d) duration of the slide, f) coherent nature of the slide, g) grain size and spectrum, h) characteristic speed of the slide.

The aim of the study is to obtain a relationship between the volume V of the slide and the maximum amplitude H of the resulting tsunami waves, based on observational data available in the published literature and to compare this relationship with the results of some numerical models. The basic argument used in the paper is that the slide volume must remain the most important basic parameter. The goal is then to obtain an order of magnitude relationship between V and H. Murty also notes that this relationship is phenomenological.

As a result, a regression line was fitted making use of observational data alone. Based on this regression the following relationships were obtained.

$$H = 0.3945V \quad (1)$$

or

$$V = 2.3994H \quad (2)$$

where V is the in millions of cubic meters and H is in meters.

Lynett and Liu (2003), derived a mathematical model to describe the generation and propagation of water waves by a submarine landslide. The model consists of a depth

integrated continuity equation and a momentum equation, in which the ground moving is a forcing function. These equations include full nonlinear, but weakly dispersive effects. Authors say that the model is also capable of describing wave propagation from relatively deep water to shallow water. A numerical algorithm is developed for the general fully nonlinear model. As a case study, tsunamis generated by prehistoric massive submarine slump off the northern coast of Puerto Rico are modeled. In the paper, the evolution of the created waves and large runup due to them is discussed.

To study the waves and runup/rundown generated by a sliding mass, a numerical simulation model, based on the large-eddy-simulation (LES) approach, was developed by Liu et al. (2004). In this study, the Smagorinsky subgrid scale model was employed to provide turbulence dissipation and the volume of fluid (VOF) method was used to track the free surfaces and shoreline movements. Authors also implemented a numerical algorithm for describing the motion of the sliding mass.
A set of large-scale experiments was conducted in a wave tank to validate the numerical model. To represent landslides, a freely sliding wedge with two orientations and a hemisphere were used. The slide mass varied over a wide range, and their initial positions ranged from totally aerial to fully submerged. The time histories of water surface and the runup at a number of locations were measured.
In the paper, comparisons between the numerical results and experimental data are presented only for wedge shape slides. Very good agreement is shown for the time histories of runup and generated waves. The detailed three-dimensional complex flow patterns, free surface and shoreline deformations are further illustrated by the numerical results. The maximum runup heights are presented as a function of the initial elevation and the specific weight of the slide. The effects of the wave tank width on the maximum runup are also discussed in the paper and given in the following:

i. The runup decreases as the submergence increases asymptotically, approaching zero as the submergence tends to infinity, for the submerged cases.
ii. Sliding hemisphere indicated larger rundown than runup for the same submergence-specific weight parameter.

iii. The runup and rundown are controlled by size, submergence and initial motion time history.
iv. When the depth of submergence is greater than three times the height of the slide, the slide becomes ineffective in generating waves.

Grilli and Watts (2005), performed numerical simulations with 2D fully nonlinear potential flow (FNPF) model for tsunami generation by two idealized types of submarine mass failure (SMF): underwater slides and slumps. The authors define slides as thin, translational failures traveling over long distances, and slumps as thick rotational failures occurring with minimal displacement. Tsunami amplitudes and runup values are obtained from the computed free surface elevations. Model results are experimentally validated for a rigid 2D slide. Sensitivity studies are performed to estimate the effects of SMF shape, type, and initial submergence depth on the generated tsunamis. A strong SMF deformation during motion is shown to significantly enhance tsunami generation, particularly in the far field. Typical slumps are shown to generate smaller tsunamis than corresponding slides. Both tsunami amplitude and runup are shown to depend strongly on initial SMF submergence depth. For the selected SMF idealized geometry, this dependence is simply expressed by power laws. The authors concluded that for rigid slides of Gaussian shape, both near and far field tsunami amplitudes increase if shape spreading decreases. Another conclusion is that a reasonable rate of deformation during motion has little effect on near field tsunami features, but more significant effects on far field features. Tsunami features computed for underwater slides and slumps of identical density and geometry. Finally the effect of initial submergence depth is studied for a rigid slide, and a detailed analysis of tsunami amplitude and runup was made. The tsunami amplitude was found to grow inversely proportional to the power 1.25 of initial submergence depth.

Harbitz et al. (2006) focused on the characteristics of a tsunami generated by a submarine landslide. These characteristics are determined by the volume, initial acceleration, maximum velocity, possible retrogressive behavior, water depth, and distance from shore. According to Harbitz et al. (2006), submarine landslides are often sub-critical (Froude number << 1), and the maximum tsunami elevation

generally correlates with the product of the landslide volume and acceleration divided by the wave speed squared. Examples of numerical simulations show that only 0.1-15 % of the potential energy released by the landslide is transferred to wave energy. Also, in the paper it is stated that tsunamis generated by submarine landslides often have very large run-up heights close to the source area, but have limited far field effects comparing to earthquake generated tsunamis. Writers exemplified these aspects by simulations of the Holocene Storrega Slide, the 1998 Papua New Guinea, and the 2004 Indian Ocean tsunamis.

Masson et al. (2006) summarize current knowledge of landslides and the problems of assessing their hazard potential. In this paper, occurrence, distribution and scale of landslides, submarine landslides and hazards, causes of landslides, landslide processes, landslide generated tsunamis, prediction and risk assessment, numerical modeling of landslide dynamics, numerical modeling of landslide tsunamis are explained. The Storrega slide and Canary Islands slides are exemplified.

Hayır et al. (2008), in their study, examined the tsunamis resulting from a submarine mass failure such as slides and slumps triggered by earthquakes or other environmental effects, which is settled at the bottom of the north eastern Sea of Marmara. The main objective of the solution method is to combine an analytical solution presenting near-field tsunami amplitudes above the submarine mass failure with a numerical solution indicating the tsunami amplitudes in the coastal regions. One common linear boundary between analytical and numerical solution domain is defined in the study. The solutions are obtained in the numerical region using TELEMAC-2D software system. In this work, Hayır et al. (2007) considered the submarine mass failure located in the north eastern Sea of Marmara. The various moving scenarios are investigated.

Kılınç (2008), in his PhD thesis, aimed to calculate the wave heights of the tsunami waves according to several scenarios resulting from the movements that might occur in the landslide area offshore Tuzla near East Marmara, İstanbul. Two types of underwater landslide simulations are done considering 400m and 800m deep slides at the landslide area at offshore Tuzla. For both landslide model time histories of the

water surface elevations above the landslide are obtained by analytical methods. These elevations are carried to the shore with the numerical method: Finite Element Method and the out time histories are obtained for points selected at the shore.
The first part of this study, landslide thickness and width are kept constant and the numerical model is run for different landslide velocities between Cr=10 m/s Cr=300m/s and the wave heights at the shore are calculated. The effects of landslide velocity and landslide model on the wave height at the shore are observed. Also, to observe the effect of dispersive and non-dispersive waves on the wave height, the equations used in the numerical model are changed. In addition to this, to obtain tsunami risk map, the maximum wave heights are calculated for selected critical points. The arrival times of the selected waves are calculated as it si important for early warning systems.

As another stage, landslide thickness and width is changed and the maximum wave heights are observed to increase as the landslide thickness and width increases.
Lastly, in his thesis study Kılınç (2008), compared the basic models with the occasions which the underwater landslide moves with acceleration.

Lopez-Venegas (2008) observed and modeled submarine landslide as the source for the October 11, 1918 Mona Passage tsunami, as a case study. A local tsunami that claimed 100 lives along the western coast of Puerto Rico was generated by the October 11, 1918 M_L 7.5 earthquake in the Mona Passage between Hispaniola and Puerto Rico. Now, the affected area is significantly more populated. A fresh submarine landslide is shown by newly acquired high-resolution bathymetry and seismic reflection lines in the Mona Passage. The authors indicate that the landslide area is approximately 76 km^2 and displaced probably a total volume of 10 km^3. Lopez-Venegas et al. modeled the tsunami as generated by a landslide with duration of 325s and with the observed dimensions and location by using the extended, weakly nonlinear hydrodynamic equations implemented in the program COULWAVE. Calculated marigrams showed a leading depression wave followed by maximum positive amplitude in agreement with the reported polarity, relative amplitudes, and arrival times. Authors suggest this newly identified landslide, which was likely triggered by the 1918 earthquake, was the primary cause of the October 11

tsunami and not the earthquake itself. Results from this study should be useful to help discern poorly constrained tsunami sources in other case studies.

With the help of these studies in literature the landslide triggered tsunami generation mechanism and landslide generated tsunamis in the Sea of Marmara are studied in the next chapters.

CHAPTER 3

LANDSLIDE TRIGGERED TSUNAMI GENERATION MECHANISM AND HISTORICAL EVENTS

During a submarine landslide, the equilibrium sea-level is altered by sediment moving along the sea-floor. Gravitational forces then propagate the tsunami given the initial perturbation of the sea-level.

The generation and propagation of landslide generated tsunamis is a complex problem. According to Harbitz et al. (2006), the problem can be divided into four parts:

1. Landslide dynamics
2. Energy transfer from landslide motion to water motion
3. Wave propagation in open water
4. Wave run-up along the shore

Underwater landslides generally occur some tens of km near the shore on the sloping bottom. The wave is usually steep and shorter in length comparing to other tsunamis. Since the distance from the shore is not so far, it directly propagates towards nearest coastline without any significant dispersion.

Harbitz et al. (2006) classifies tsunamis generated by submarine landslides as long waves as most of the energy transferred from the landslide to the water motion is distributed on waves with typical wavelengths much larger than the characteristic water depth.

Okal and Synolakis (2003) simplify underwater slumps by considering a mass of solid mass along the sea bottom and the moving slide creates a bulge resulting in a

positive source at the toe, while leaving a mass deficiency at its heel. As a result, the sea surface takes a dipolar character (Figure 3.1).

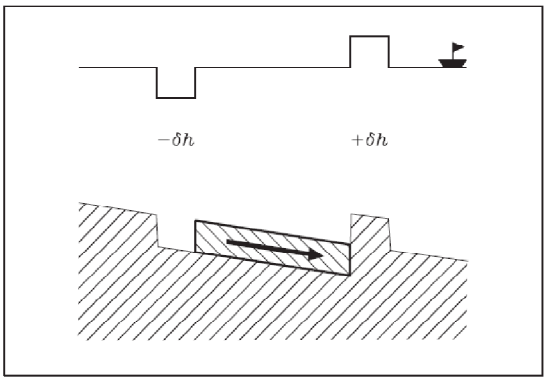

Figure 3.1: Generation of A Tsunami Wave by an Underwater Slide (Okal and Synolakis, 2003)

Figure 3.2 illustrates tsunami wave generated by a bulge moving at velocity V slower than Celerity (V<C). After the motion starts tsunami wave develops ahead of the deformation, while a smaller wave propagates in the opposite direction (b). The motion stops at t=T (c) and the tsunami waves propagating outwards and backwards have the structure of a dipole (Okal and Synolakis, 2003)

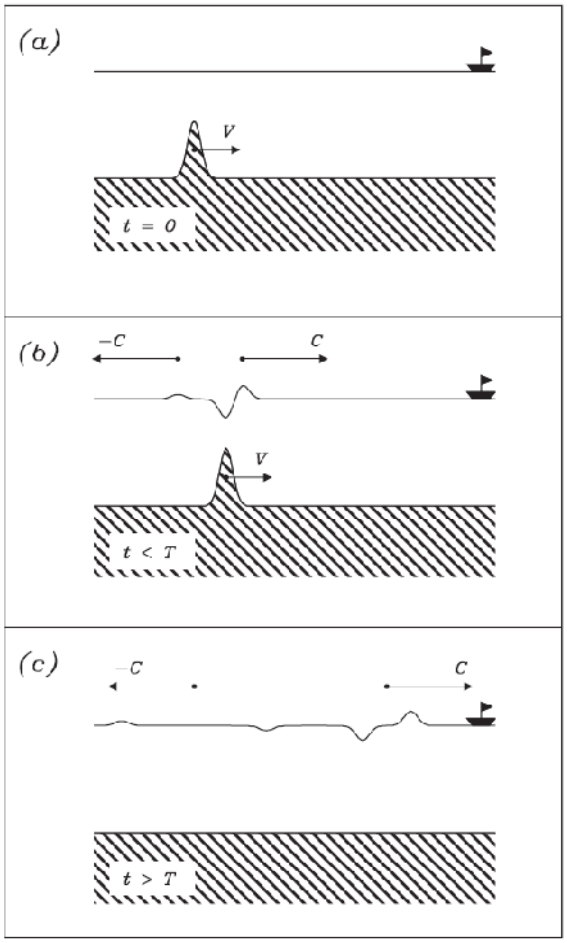

Figure 3.2: Tsunami Wave Generated By a Bulge Moving On the Ocean Floor at Velocity V (Okal and Synolakis, 2003)

Radial spreading of landslide generated tsunamis from a local dipole source results in large run-up heights close to the landslide area and limited far field effects (Harbitz et al. 2006). Hence, it causes major impact at the shorter distance of coastline but during its long distance propagation its energy disperses and wave amplitude decreases.

The total volume of the slide material is expected to be the main parameter which affects the amplitude of a tsunami generated by a submarine landslide even though several other parameters also play important roles (Murty 2003). The definition

sketch of the landslide generated tsunami parameters are given in Figure 3.3 and some of these parameters are given in the following:

a) Volume of slide

b) Thickness of the slid material

c) Characteristic speed with which the slide moves OR

c.1) Total distance moved by the slide

c.2) Duration of the slide

d) Acceleration

e) Depth of water above slide

f) Angle of the slide from the horizontal (or vertical) direction.

g) Density of the slide material

h) Coherent nature of the slide

i) Grain size

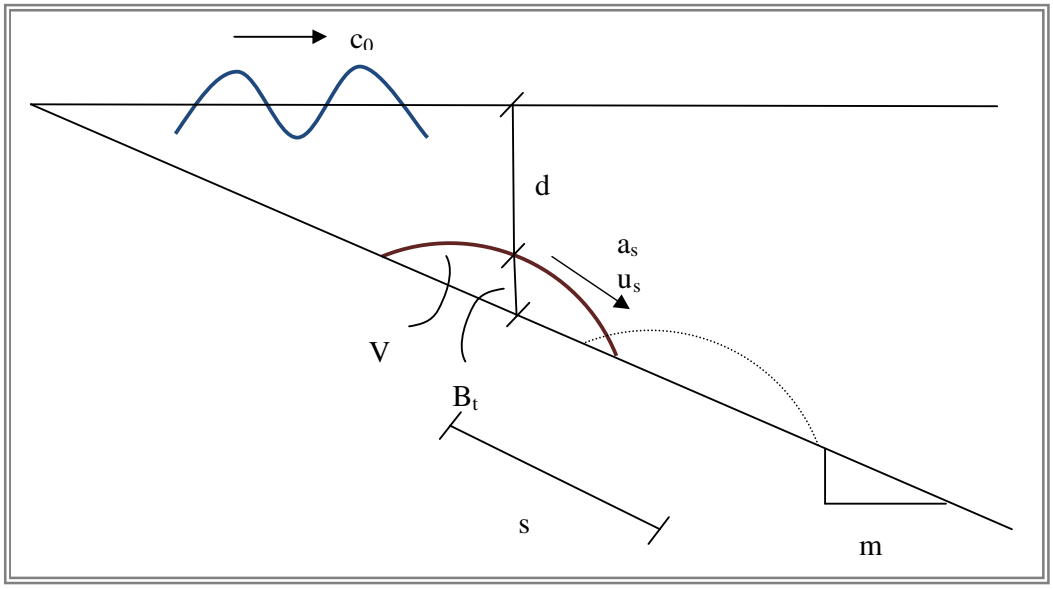

Figure 3.3: Definition Sketch, Landslide Generated Tsunami Parameters

c_0 : linear long wave speed, $\sqrt{gh}$

u_s: speed of slide

a_s: acceleration of slide

d: depth of water above the slide

V: volume of the slide

B_t: thickness of the slide

m: slope of the landslide location

s: slide distance

t: time

The relation between the volume of the slide and the maximum water elevation is studied by many scientists. Harbitz et al. (2006) state that the maximum surface elevation generally correlates with the product of the **volume** of the slide and **acceleration** divided by wave speed squared for strongly sub-critical landslide motion, i.e., the Froude number is much less than one. The writers define Froude number as $Fr = u/c_0$ where u is the landslide speed.

Considering a block with uniform thickness moving on a horizontal seabed with constant velocity and ignoring dispersion, the demonstrations showed that the **length** of the sliding block affects the wave length, and the **thickness**, **velocity** and **wave speed** (depends on **water depth**) of the slide affects surface elevation.

Fine et. al. (2003) investigated the effect of the **depth of water above the slide**. The results were surprisingly different for rigid-body and viscous slides. For rigid body slides, the tsunami waves are more energetic when the initial slide above sea level is greater. However, for viscous slides, there is an optimal slide height, which produces largest tsunami waves. Slides initially located above or below this position, located close to the coastline, generate less energetic waves. The total wave energy as functions of slope angle and the initial slide position for rigid body and viscous slides are given in Figure 3.4.

Figure 3.4 also gives results for **slope angle**. Slope angle range from 2° to 10° gives identical results for rigid body and viscous slides. The steeper the slopes, the higher the generated surface waves (Fine et al., 2003).

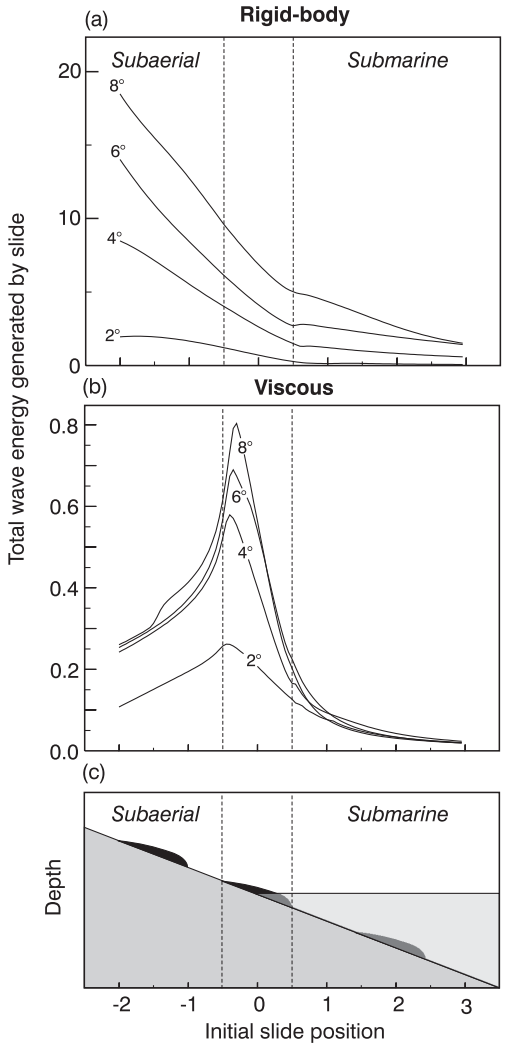

Figure 3.4: Total Wave Energy as Functions of Slope Angle and the Initial Slide Position (c) For: (a) Rigid Body Slide, and (b) Viscous Slide (Fine et al., 2003).

Historical Events

There are several tsunami events generated by landslides in history. These events are listed below and brief information about these landslide generated historical tsunamis is given.

- **Storegga Slides I,II,III tsunami(s) (30000 yr B.P, 9000 yr, 7000-8000 yr B.P)**
  There are many studies exemplifying Storrega slides. Storegga slide, which is probably initiated by an earthquake, on the Norwegian continental slope has induced tsunami waves between Scotland and Norway. The slide, which ended up at a depth of 300-2500 metres, created a 10-20 meters high tidal wave that reached the Norwegian coast.The Storegga submarine slides occurred on the continental slope off the coast of western Norway (Figure 3.5), extending out into the Norwegian Basin. There were three slide events: the first slide occurred approximately 30,000-35,000 years before present (2). The second and third slides occurred very close together at approximately 7,000 years before present (2). It is stated that earthquakes possibly together with gas released from the decomposition of gas hydrates are considered to be the most likely triggering mechanisms for the slides (Jansen, 1987 in Yalciner et. al., 2005).

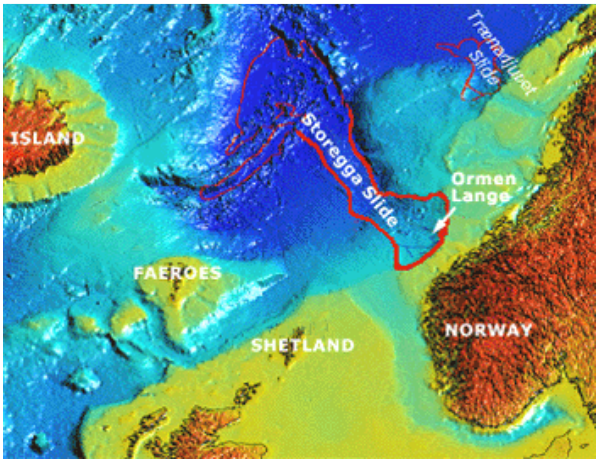

Figure 3.5: The Ormen Lange field is located close to the steep back edge of the Storegga slide, which 8100 years ago ended up at a depth of 300-2500 meters (http://www.ormenlange.com/en/about_ormen/key_features/storegga_slide/)

- **1894 Tacoma**

  Bornhold et al. (2001) state that at the inlets and narrow straits of the pacific coasts of North America (e.g. Lituya Bay, Yakutat, Russel Fjord, Skagway Harbor, Kitimat Arm, Tacoma) landslide generated tsunamis occur frequently and have large runup values. The locations of major coastal and underwater landslides which triggered tsunamis around British Columbia are shown in Figure 3.6.

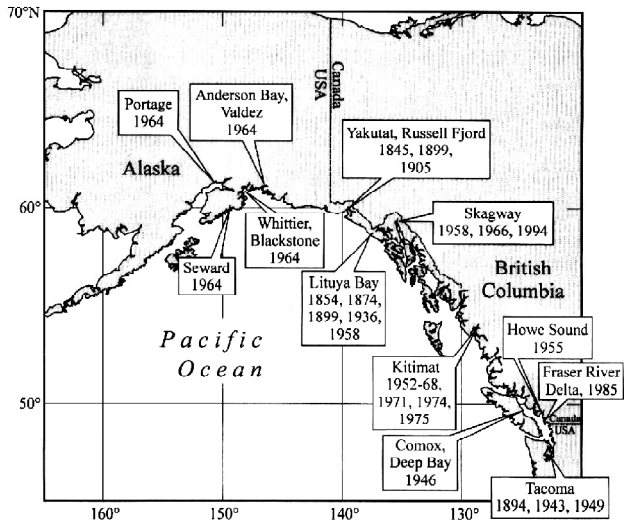

Figure 3.6: Locations and Dates of Major Coastal and Underwater Landslides Which Triggered Tsunamis around British Columbia (Bornhold et. al., 2001)

- **1918, October 11th – Mona Passage**

  A local tsunami was generated by a 7.5 magnitude earthquake which claimed 100 lives along the western coast of Puerto Rico. The high resolution bathymetry and seismic reflection lines show that a submarine landslide occurred which has an area of approximately 76m^2 and a total volume of 10km^3 (Lopez-Venegas et al, 2008).

- **1929, November 18 - The Grand Banks, Newfoundland.**

  According to Ward and Day (2002), between 300 and 700 km^3 of sediment slid off and plunged into the depths of the Atlantic at speeds near 80 km/h. During the event, the landslide mass turned into a giant flow of turbulent and broke several transatlantic telegraph cables connecting America and Europe. Waves of 10m claimed nearly 30 lives.

- **1946, April 1 - Unimak Island (Aleutian Islands)**

  The Unimak (eastern Aleutians) earthquake of April 1, 1946 (MS =7.1) produced a large tsunami (Mt =9.3) which killed 167 people (Fryer et al., 2004) (See Figure 3.7). The narrow beam of large waves in the far field and the rapid variation in near-source runup could not be explained by only seismic source. According to the writers, the slow rupture, the tsunami directivity, the rapid variation in near-source wave heights, the period of the waves, suggest an earthquake-triggered landslide. The depth of the slide is estimated as 120 m, while the dimensions being 25 km across, 65 km long, and having a volume of 200-300 km^3.

Figure 3.7: Scotch Cap Coast Guard Station, Unimak Island, Before and After the Tsunami (Fryer Et Al., 2004)

- **1952-1974 - Kitimat**

  (See 1894 Tacoma part)

- **1956, July 9 – Amorgos Island, Greece**

  The earthquake of magnitude 7.8 was the largest one to strike Greece in the 20th century, near Amorgos Island in the southcentral Aegean Sea, It resulted in 53 deaths and considerable damage, notably on the island of Santorini, and generated a local tsunami affecting the shores of the Cyclades and Dodecanese Islands, Crete and the Turkish coast of Asia Minor, with run-up values of 30, 20, and 10 m reported on the southern coast of Amorgos, on Astypalaia and Folegandros, respectively. High values reported in the 20th century over the whole Mediterranean Basin led later to propose a submarine landslide (or a series of landslides) as the source of the tsunami, based on the excessive amplitude and general heterogeneity of run-up in the epicentral area (Okal et. al., 2009).

- **1958, July 9 - Lituya Bay, Alaska**

  The event causing maximum runup heights of more than 500m was a result of rock slide (Harbitz et al., 2006).

- **1964, Mar 28 - Prince William Sound, Alaska.**

  Lee et. al (2006) investigated the The Great Alaska Earthquake of 1964. Acoording to the paper, the natural event caused major damage and 43 deaths in the coastal communities of Seward and Valdez. Most of these losses were caused by tsunamis that occurred immediately after the earthquake and were most likely induced by local submarine landslides. It is stated that, landslide deposits near Seward typically take the form of a series of large and small blocks lying directly off the front of the town, although there are indications of sandy and muddy debris flows occurring off river deltas. The 1964 landslide tsunamis may have been composites resulting from a number of landslide events.

- **1979, Oct 16 - Nice, France**

  On the 16th of October 1979, a part of the Nice new harbor extension, close to the Niceinternational airport (French Riviera), slumped into the Mediterranean Sea during landfilling operations. According to Assier-Rzadkiewicz et al., (2000) a submarine slide with initial volume close to seashore of about 10 millions m3,

was followed by a small tsunami, noticed by several witnesses in the ‘‘Baie des Anges.’’ The maximum tsunami effects were observed 10 km from the slide location near Antibes city, which was inundated.

- **1992 – Flores Island, Indonesia**
  Tsunami waves with heights up to 26m associated with an earthquake of magnitude Ms= 7.5 (Bornhold et. al, 2001)

- **1994, November 3rd - Skagway Harbor, Southeast Alaska**
  3-10 x 106 m3 of loose alluvial sediment slid down the fjord at various locations within Taiya inlet. Since no seismic activity was recorded, the slide may have been triggered by a number of factors, including an exceptional low tide, recent rip-rap overburden and pile removal operations, artesian water flow, and recent sedimentation from the Skagway River. The event caused a tsunami that destroyed most of a railway dock and claimed 1 life (Watts et. al, 2005).

- **1998, July 17th - Papua New Guinea**
  Although, at first it was believed that the tsunami originated from an earthquake, the results of the model of the tsunami gave too small amplitudes and too late arrival times showed that the damaging part of the tsunami was due to a slump. There were 2200 casualties due to run-up heights up to 15m affecting a 20 km segment of the coast (Harbitz et al. 2006). Recent investigations suggest that the underwater slump involved 4 km^3 of sedimentary material and occurred 13 minutes after the main shock and generated exceptionally high runup on the local coast and minimal at transpacific distances (Okal and Synolakis, 2003).

- **1999, August 17th- İzmit**
  During İzmit earthquake the ground motion caused mass movements within coastal zones of İzmit Bay. Submarine sliding of slumped blocks generated sea-surface oscillation, that generated tsunamis that caused flooding and destruction upon coasts (Alpar et al., 2000). The disaster took close to 20,000 lives and left more than 100,000 people homeless. In Değirmendere town (south of İzmit bay) the triangular shape (220 m along shore and 80 m perpendicular to shore) of

coastal alluvial headland slid and the depth became 15 m in average in the slide location (Yalciner et. al., 2001).

- **1999, Sep 15th - Fatu Hiva, Marquesas Islands**

  On 13 September 1999, a local tsunami, comprising two waves separated by a few minutes, hit the village of Omoa, on the island of Fatu Hiva, French Polynesia. The tsunami caused serious damage to the coastal structures at the area. The tsunami was generated by a collapse of a basaltic cliff located to the southeast of Omoa. The volume of the landslide is estimated in range from 2 to 5 million m3 of which 60 % fell into the sea (Okal et. al., 2002).

- **2002, December 30 – Stromboli**

  Stromboli is one of the two active volcanoes in the southern Tyrrhenian sea. On December 30 2002, a massive submarine landslide, followed by a subaerial one detached from the island producing a tsunami. Many buildings were severely damaged. The total volume of the slid material was about 20,000,000 m^3 (Maramai et al 2005).

CHAPTER 4

MODELING OF TSUNAMIS GENERATED BY SUBMARINE LANDSLIDES

Since there are several parameters affecting the wave generation by submarine landslides (See Chap. 3), the modeling of tsunamis generated by submarine landslide is a complex issue. Numerical modeling of tsunamis caused by submarine landslides is a much more complicated problem than simulation of earthquake generated tsunamis. According to Fine et al. (2003) that is because the durations of the slide deformation and propagation are adequately long that they affect the characteristics of the surface waves. Therefore, coupling between the slide body and the surface waves must be considered. In addition to this, the landslide shape changes significantly during sliding and that causes change in the surface waves it generated.

As a computational approach, the numerical model TWO-LAYER, developed in Tohoku University, Disaster Control Research Center by Prof. Imamura, can be used for modeling (Imamura and Imteaz (1995), Ozbay (2000), Yalciner et al (2002)).

If mud and water are considered two different layers of flow, two-layer long waves or flows (like the surface wave and mudslide) can also be applied in the case of underwater landslides. Therefore, the interaction between each layer should also be considered as different from the one-layer models. Two-layer flow may result from density differences within the fluid. In two-layer flow both layers interact and play a significant role in the establishment of control of the flow. The effect of the mixing or entrainment process at a front or an interface becomes important. The reliability and accuracy of the two-layer model is verified through the comparison with the analytical solution under simplified conditions by Imamura and Imteaz (1995).

4.1 Theoretical Approach

Two-layer flows that occur due to an underwater landslide can be modeled using a non-horizontal bottom with a hydrostatic pressure distribution, uniform density distribution, uniform velocity distribution and negligible interfacial mixing in each layer. The schematic view of two-layer flow is shown in Fig. 4.1. Conservation of mass and momentum can be integrated in each layer, with the kinetic and dynamic boundary conditions at the free surface and interface surface (Imamura and Imteaz (1995).

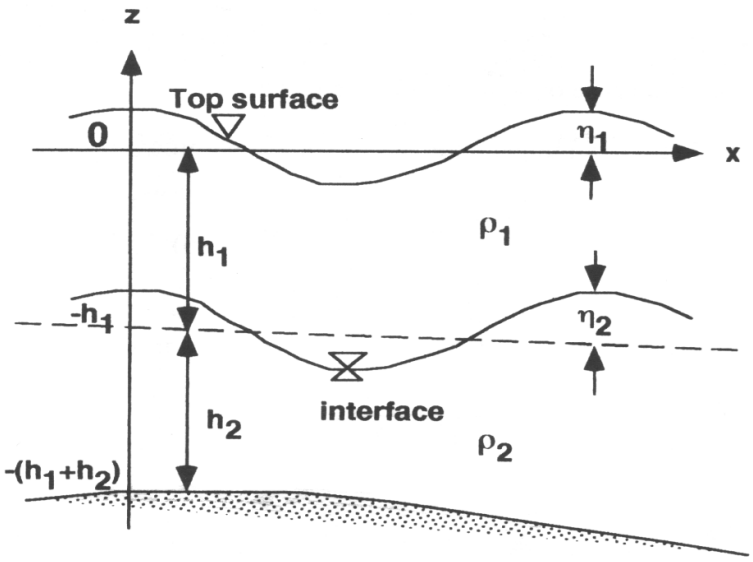

Figure 4.1: Definition Sketch for Two-Layer Profile (Imamura and Imteaz (1995)

Governing equations for the upper layer are given in the following and the derivation procedure is summarized in Imamura and Imteaz (1995).

$$\frac{\partial(\eta_1-\eta_2)}{\partial t}+\frac{\partial M_1}{\partial x}+\frac{\partial N_1}{\partial y}=0 \tag{4.1}$$

$$\frac{\partial M_1}{\partial t}+\frac{\partial\left(\frac{M_1^2}{D_1}\right)}{\partial x}+\frac{\partial\left(\frac{M_1N_1}{D_1}\right)}{\partial y}+gD_1\frac{\partial\eta_1}{\partial x}-gD_1\frac{\partial\eta_2}{\partial x}+\frac{g\eta^2}{D_1^{7/3}}M_1\sqrt{M_1^2+N_1^2}=0$$

(4.2)

$$\frac{\partial N_1}{\partial t}+\frac{\partial\left(\frac{N_1^2}{D_1}\right)}{\partial y}+\frac{\partial\left(\frac{M_1N_1}{D_1}\right)}{\partial x}+gD_1\frac{\partial\eta_1}{\partial y}-gD_1\frac{\partial\eta_2}{\partial y}+\frac{g\eta^2}{D_1^{7/3}}N_1\sqrt{M_1^2+N_1^2}=0$$

(4.3)

and those for the lower layer are:

$$\frac{\partial\eta_2}{\partial t}+\frac{\partial M_2}{\partial x}+\frac{\partial N_2}{\partial y}=0$$

(4.4)

$$\frac{\partial M_2}{\partial t}+\frac{\partial\left(\frac{M_2^2}{D_2}\right)}{\partial x}+\frac{\partial\left(\frac{M_2N_2}{D_2}\right)}{\partial y}+gD_2\left\{\alpha\left(\frac{\partial\eta_1}{\partial x}+\frac{\partial h_1}{\partial x}-\frac{\partial\eta_2}{\partial x}\right)+\frac{\partial\eta_2}{\partial x}-\frac{\partial h_1}{\partial x}\right\}+\frac{g\eta^2}{D_2^{7/3}}M_2\sqrt{M_2^2+N_2^2}=0$$

(4.5)

$$\frac{\partial N_2}{\partial t}+\frac{\partial\left(\frac{N_2^2}{D_2}\right)}{\partial y}+\frac{\partial\left(\frac{M_2N_2}{D_2}\right)}{\partial y}+gD_2\left\{\alpha\left(\frac{\partial\eta_1}{\partial y}+\frac{\partial h_1}{\partial y}-\frac{\partial\eta_2}{\partial y}\right)+\frac{\partial\eta_2}{\partial y}-\frac{\partial h_1}{\partial y}\right\}+\frac{g\eta^2}{D_2^{7/3}}N_2\sqrt{M_2^2+N_2^2}=0$$

(4.6)

Where η is the surface elevation, D=h+ η the total depth, h is the still water depth, M and N are the discharge fluxes in x and y directions respectively, ρ the density of the fluid, $\alpha=\rho_1/\rho_2$, and subscripts 1 and 2 indicate the upper and lower layer respectively (Imamura and Imteaz, (1995)). M_1, N_1, η_1, η_2, M_2, N_2 are solved from the above 6 equations numerically. At the open boundary the total derivative of surface elevation is set to be equal to zero as:

$$\frac{D\eta}{Dt}=0 \qquad (4.7)$$

The dynamic and kinetic boundary conditions at surface and bottom are given as follows:

$$p = 0 \qquad at\ z = \eta \qquad (4.8)$$

$$w = \frac{\partial \eta}{\partial t} + u\frac{\partial \eta}{\partial x} + v\frac{\partial \eta}{\partial y} \qquad at\ z = \eta \qquad (4.9)$$

$$w = -u\frac{\partial h}{\partial x} - v\frac{\partial h}{\partial y} \qquad at\ z = -h \qquad (4.10)$$

4.2 Numerical Approach

The staggered leap-frog scheme (Shuto, Goto, Imamura, (1990)) has been used to solve the governing equations for long waves numerically. This scheme is one of explicit central difference schemes. The staggered scheme considers that the computation point for one variable, η, does not coincide with the computation point for other variable, M. There are half step differences, 1/2Δt and 1/2Δx between computation points of two variables. Thus one variable, η, is placed at the middle of Δt Δx rectangle, placing other variables at the four corner of rectangle and vice versa. In the finite difference formulation 'n' denotes the temporal grid points and 'i' and 'j' denote the spatial grid points along x and y directions. Δx, Δy, and Δt are spatial grid spacings and time step respectively. Using this scheme, the finite difference equations for the governing equations are obtained (Imamura and Imteaz, (1995)).

In spatial direction, all of η_1, η_2 at step 'n+ ½' and all of M_1, M_2 at step 'n' are given as initial conditions. For all later time steps at left and right boundaries, all values of either discharge or water elevation would be calculated by using the values of previous time step or estimated wave celerity. This solution contains two progressive waves with different celerities and one reflective wave. By using the mass continuity equation for a lower layer, all η_2 at step 'n+3/2' are calculated and then all η_1 at step 'n+3/2' for an upper layer are calculated using latest values of η_2. Then, using the

momentum equation for an upper and a lower layer, all values of M_1, N_1, M_2, N_2 at step 'n+1' are simultaneously calculated. Similarly, using new values of η_1, η_2, M_1, N_1, M_2, N_2 as initial values for the next time step, the calculations proceeds in time up to desired step.

While doing these calculations, it is very difficult for the model to derive a stability condition analytically due to the interactions between two layers. For this purpose Courant-Friedrichs-Lewys (CFL) condition is applied where two celerities exist as one for a progressive wave and one for reflected wave. Stability is initially investigated for some arbitrary Δx and Δt. This result suggests that the model is stable up to a certain limit of $\Delta x/\Delta t$ and this limit varies with the variation of α and β (Imamura and Imteaz (1995)) as verified with different test results obtained during the preparation of this thesis for different values of α (ratio of density of fluid in an upper layer to a lower one) and β (ratio of water depth in a lower layer to an upper one). It is suggested by Imamura and Imteaz (1995) that as for lower 'α' and for higher 'β', an amplification of a top surface increases and vice versa. According to Imamura and Imteaz (1995), for α=0.5 and β=4.0, celerity of top surface calculated through analytical expression, $c_2=\left[\sqrt{gh_2(1-\alpha)/(1+\alpha\beta)}\right]$ controls the stability criteria, while for α=0.4 and β=1.0, celerity of interface $c_1=\left[\sqrt{gh_1(1+\alpha\beta)}\right]$ corresponds to the stability criteria. It is suggested by Imamura and Imteaz (1995) to consider the maximum of c_1 and c_2, to satisfy the stability condition $\Delta t \leq \Delta x/\max(c1, c2)$.

As a case study the model is applied to the landslides in the Sea of Marmara.

CHAPTER 5

UNDERWATER LANDSLIDES IN THE SEA OF MARMARA

After devastating August 17, 1999 İzmit earthquake, numerous seismic and geological studies and marine surveys have been performed in the Sea of Marmara.

Since landslide generated tsunamis have stronger effects on the nearest coastal areas and if the size and the boundaries of the Sea of Marmara is considered, the effects of a landslide tsunami may be hazardous at some locations in this enclosed sea. Landslides are often triggered by earthquakes and North Anatolian Fault can be an important factor for the generation of a landslide in the Sea of Marmara. Also, the coastline is highly utilized (especially in İstanbul) and there are several ports, coastal structures and and industrial areas along the coast of the Sea of Marmara. Therefore, the risk assessment and mitigation studies are necessary for tsunami occurrence probability.

The general characteristics of the underwater landslides in the Sea of Marmara are evaluated in the next sections.

5.1 General Characteristics of the Underwater Landslides in the Sea of Marmara

The vulnerable slopes in Marmara Sea are identified by topographical analysis during project “Simulation and Vulnerability Analysis of Tsunamis Affecting the Istanbul Coasts” (OYO and IMM, 2007). Using the bathymetry information in Marmara Sea, stereoscopic data, geological and soil information, tectonics information along North Anatolian Fault; vulnerable landslides in Marmara Sea in

the past and current that may generate tsunami are identified and 10 sites are selected as the typical vulnerable or unstable landslide sites (OYO and IMM, 2007). in Figure 5.1 the location of 10 submarine landslide sites are shown. In Table 5.1 areas, volumes and some other properties of these sites are given.

Three of these landslide sites are defined as the locations of past landslide sites in the se of marmara. They are,

a) WR1912; at western side in Tekirdag Basin reproducing the slip due to the 1912 Ganos earthquake

b) ER1509; at eastern side in Northern Cinarcik Basin reproducing the slip due to the 1509 earthquake

c) OR1894; at eastern side in Southern Cinarcik Basin for opposite side to Istanbul reproducing the slip due to the 1894 earthquake.

The other seven sites are determined as vulnerable or currently unstable areas which are estimated as probable slips due to future earthquakes;

d) WN; western side in Tekirdag Basin

e) CN; central portion in Central Basin

f) EN1; eastern side in Northern Cinarcik Basin

g) EN2; eastern side in Northern Cinarcik Basin

h) EN3; eastern side in Northern Cinarcik Basin

i) ON1; opposite side of Istanbul in Southern Cinarcik Basin (location is similar to the above OR1894 site)

j) ON2; opposite side of Istanbul in Southern Cinarcik Basin

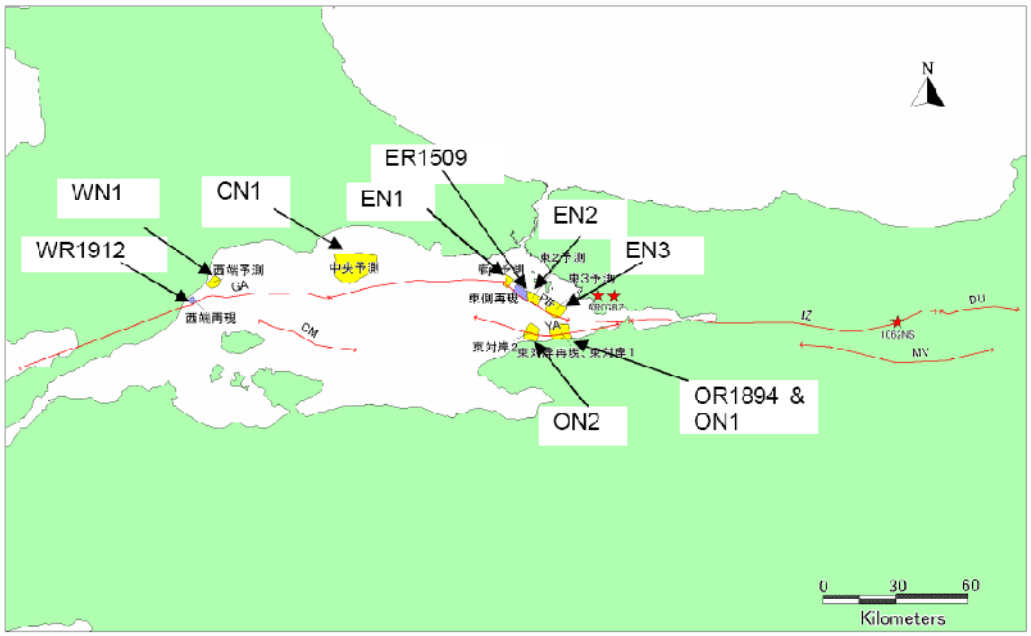

Figure 5.1: Location of Selected Vulnerable Slopes in Marmara Sea (OYO and IMM, 2007)

Table 5.1: Summary of Shapes for the Selected Slopes (OYO and IMM, 2007)

Slope	Area (sqkm)	Volume (cubic km)	Average thickness (m)	Max thickness (m)	Average inclination (deg)
OR1894	14.9	2.054	137.7	377	14.6
ER1509	12.1	0.664	55	129	19.3
WR1912	4.8	0.089	18.5	43.5	17.2
CN1	153.7	14.379	93.6	317	5.1
EN1	7.1	0.608	86	225.4	11.3
EN2	12.8	0.848	66.1	140	13
EN3	18.7	1.827	97.5	213	13.5
ON1	29.2	2.982	102.3	229.9	10.8
ON2	11.2	0.648	57.8	139.7	13
WN1	15.9	1.167	73.6	176	14

It is seen from the Table 5.1 that the maximum area and volume of landslide is in the case of CN1 and average thickness is in the case of OR1984. Among these landslide sites the underwater landslide Yalova (ON1) is selected for modeling.

5.2 Modeling of Underwater Landslide Offshore Yalova (ON1)

OR1894 is located at eastern side in Southern Çınarcık Basin for opposite side to Istanbul reproducing the slip due to the 1894 earthquake. The eastern portion of the slope shows large scale slipped topography. Among the slopes, it shows the most significant slide topography composed of steep slipped cliff, relatively gently inclined slipped mass, and small scale slipped shapes inside of slipped mass etc. The front end of slope can be clearly traced and shows a convex shape comparing with neighboring slopes end.

ON1 is located at opposite side of Istanbul in Southern Çınarcık Basin. This is the upper portion of the past landslide site of "OR1894". The landslide is estimated including the portion of the past landslide eroded mass of "OR1894".

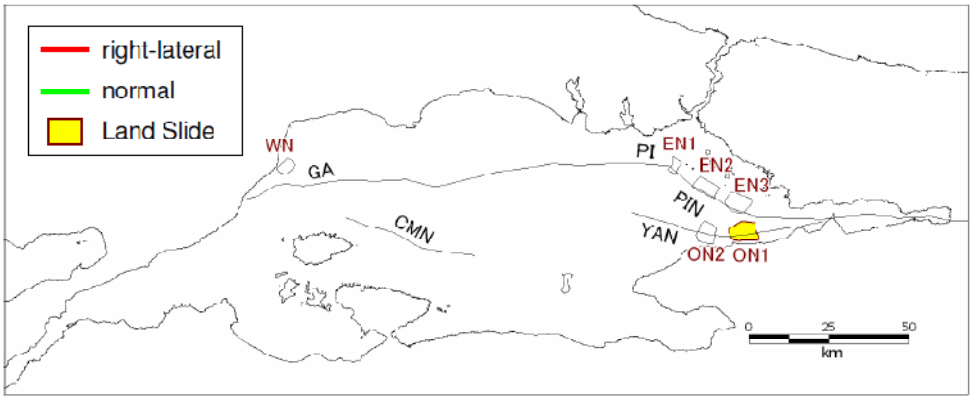

Figure 5.2: Location of the Landslide at Offshore Yalova (ON1) (OYO and IMM, 2007)

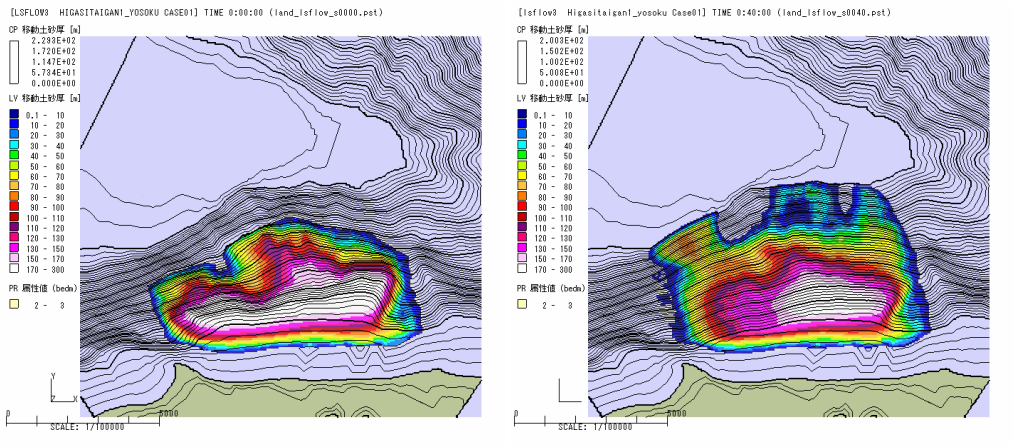

Figure 5.3: Close Up Figure of On1 Landslide and Its Initial (left) and Final (right) Thickness Distribution (OYO and IMM, 2007).

The 2D and 3D views of study domain used in the modeling of ON1 landslide are shown in Figures 5.4 and 5.6. The domain is bounded by 326233 - 458299 longitudes and 4495471.5 – 4555547 latitudes according to ED 50 (European Datum 1950). The grid size is selected as 50 m in modeling, hence the domain matrix size is 881 x 401.

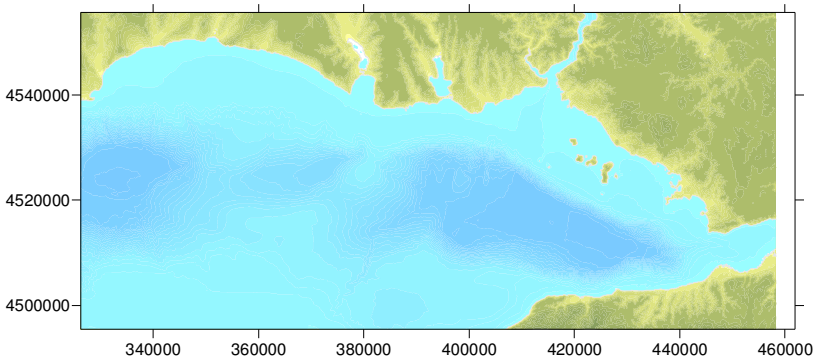

Figure 5.4: 2D View of the Study Domain Used in the Modeling of ON1 Landslide

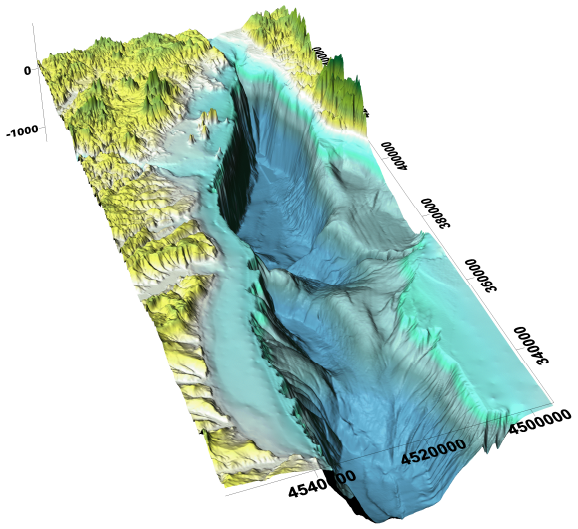

Figure 5.6: 3D View of the Study Domain Used in the Modeling of ON1 Landslide

In order to evaluate the evolution of the wave along south-north direction 178 gauge points with 50m intervals are selected along the longitude 431885.9 m, from 4502530.3 m to 4529113.7m latitudes. These gauge points form a cross section shown in red dots in Figure 5.7 along S-N direction. The cross sectional view is also shown in Figure 5.8.

The simulation of the landslide case ON1 is performed by using TWO LAYER model. The evolution of the tsunami wave according to the landslide is computed by simulating the phenomenon up to 5 minutes (until the landslide termination). The time step is selected as 0.005 seconds in order to satisfy stability. The landslides induced tsunami wave and its propagation in 1, 3, 5 minutes are shown in Figures 5.9.a, 5.9.b and 5.9.c, respectively. It can be seen that the uplift and subsidence of water surface are consistent with the Figure 3.1.

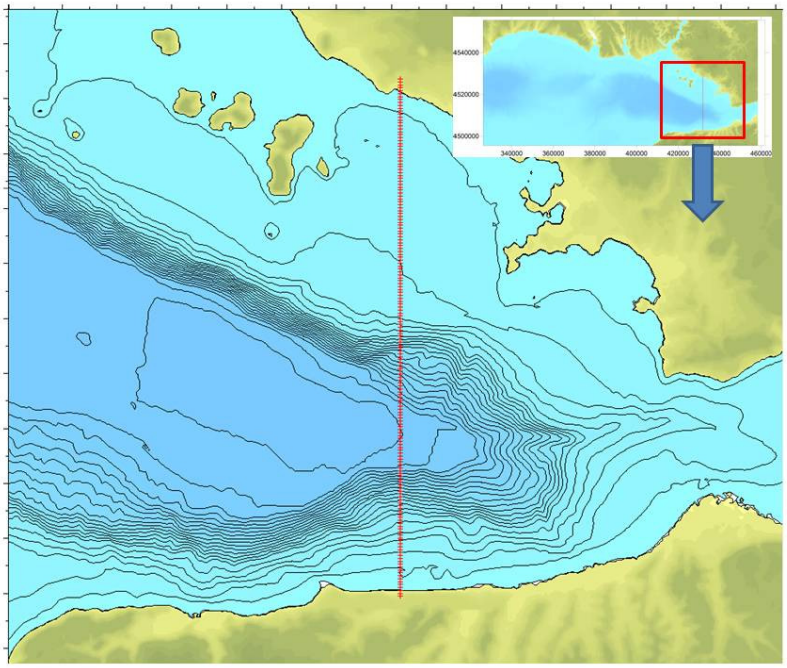

Figure 5.7: Depth Countours and the Locations of the Gauge Points along the Cross Section

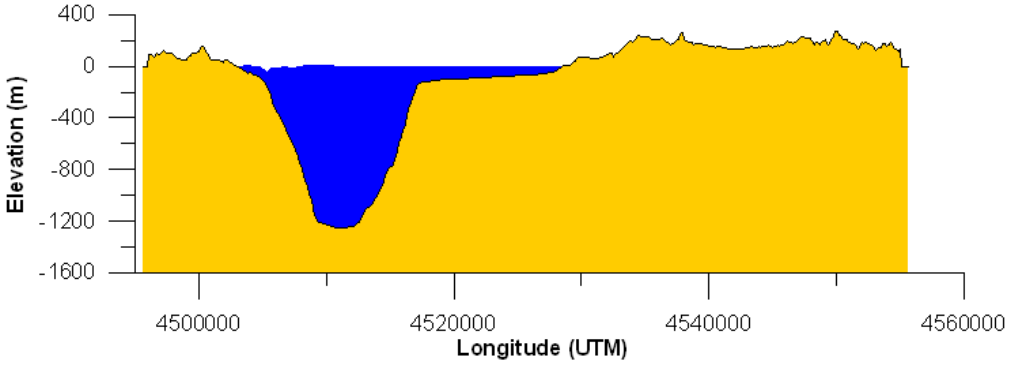

Figure 5.8: Sectional View of the Marmara Sea along S-N Direction at the Landslide Area.

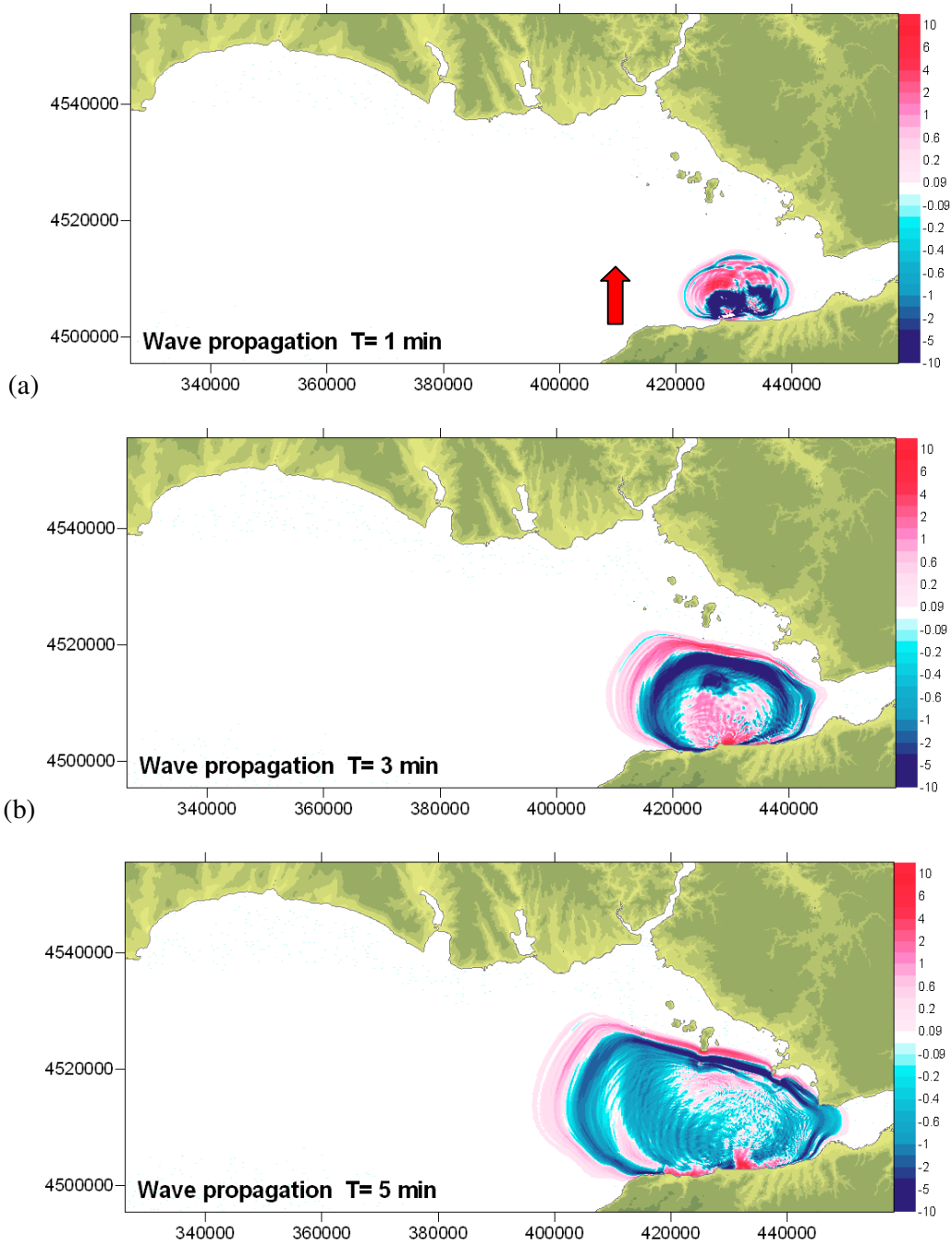

Figure 5.9: The Sea State after 1(a), 3(b) and 5(c) Minutes from the Initiation of the Landslide (The Red Arrow Represents The Direction Of The Landslide).

In the two layer flow, the density and ratio between slid material and water is important. In the following the effect of density of the slid material on the generated wave characteristics are studied.

5.2.1 Effect of density of the slid material on tsunami generation

In order to understand the effect of the density of the slid material on the tsunami generating landslide event several density values are used representing the mud density. Density of the slid material is selected as 1.2, 1.6, 2.0 ton/m^3, respectively. Figure 5.10 represents the state of the water surface along the cross section during at time steps 60 (a), 120 (b), 180 (c), 240 (d), and 300(e) seconds, respectively. As seen in the figures denser material results in maximum wave heights. It can be estimated that rock slides are more dangerous that mud slides. The figures also reveal that there is no difference in arrival times of the waves generated by landslides which have different mud densities. The propagation of the wave is similar because it is mainly dependent on the water depth.

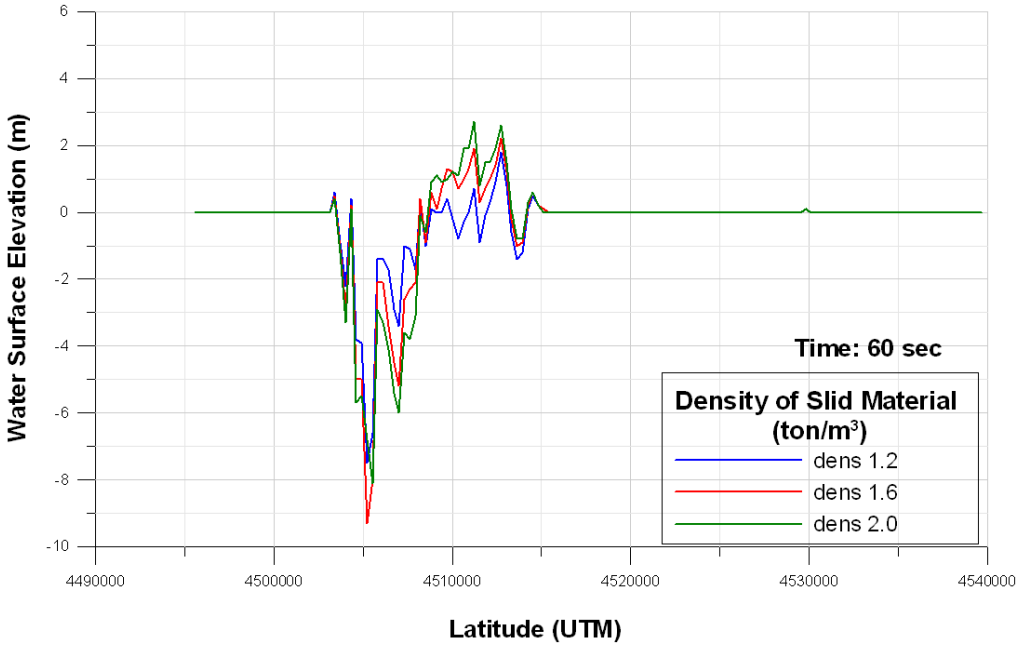

(a)

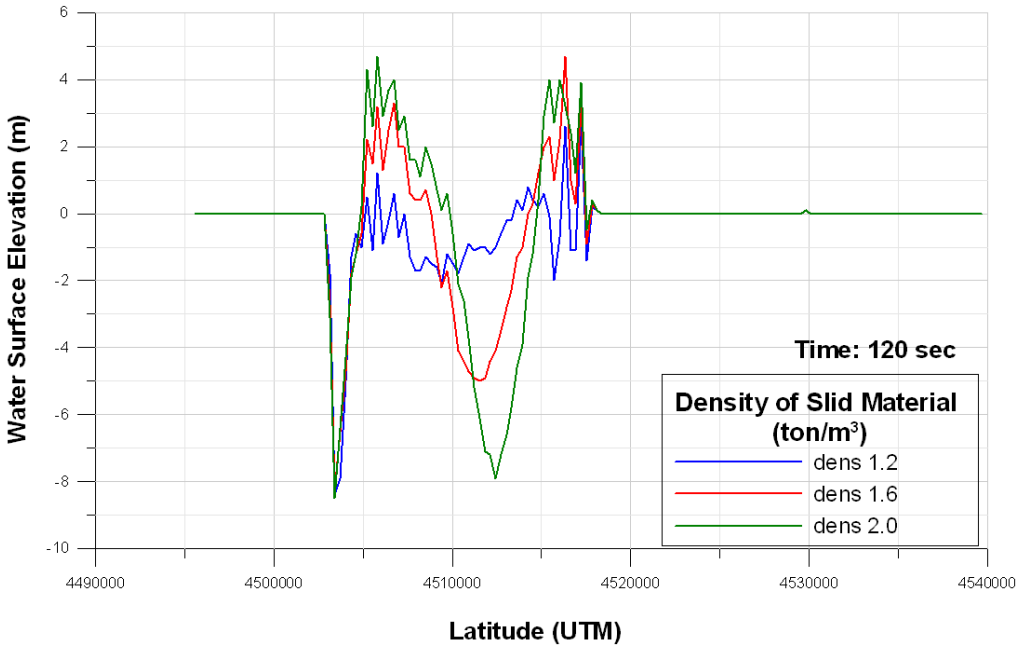
Water Surface Elevation (m)
6
4
2
0
-2
-4
-6
-8
-10
4490000
4500000
4510000
4520000
4530000
4540000
Latitude (UTM)
Time: 120 sec
Density of Slid Material (ton/m³)
dens 1.2
dens 1.6
dens 2.0

(b)

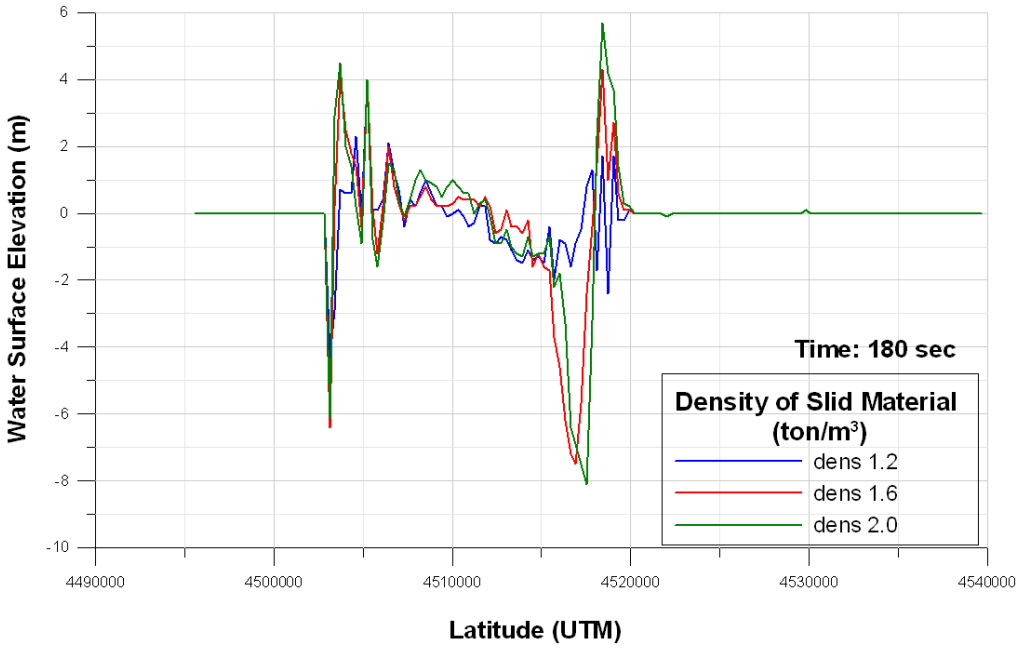
Water Surface Elevation (m)
6
4
2
0
-2
-4
-6
-8
-10
4490000
4500000
4510000
4520000
4530000
4540000
Latitude (UTM)
Time: 180 sec
Density of Slid Material (ton/m³)
dens 1.2
dens 1.6
dens 2.0

(c)

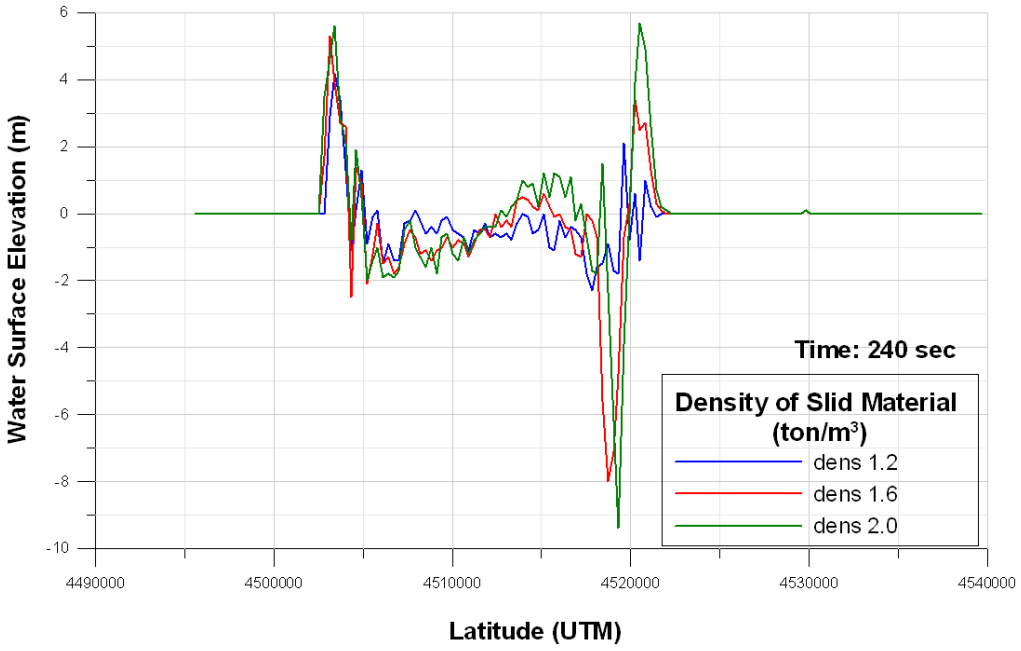

(d)

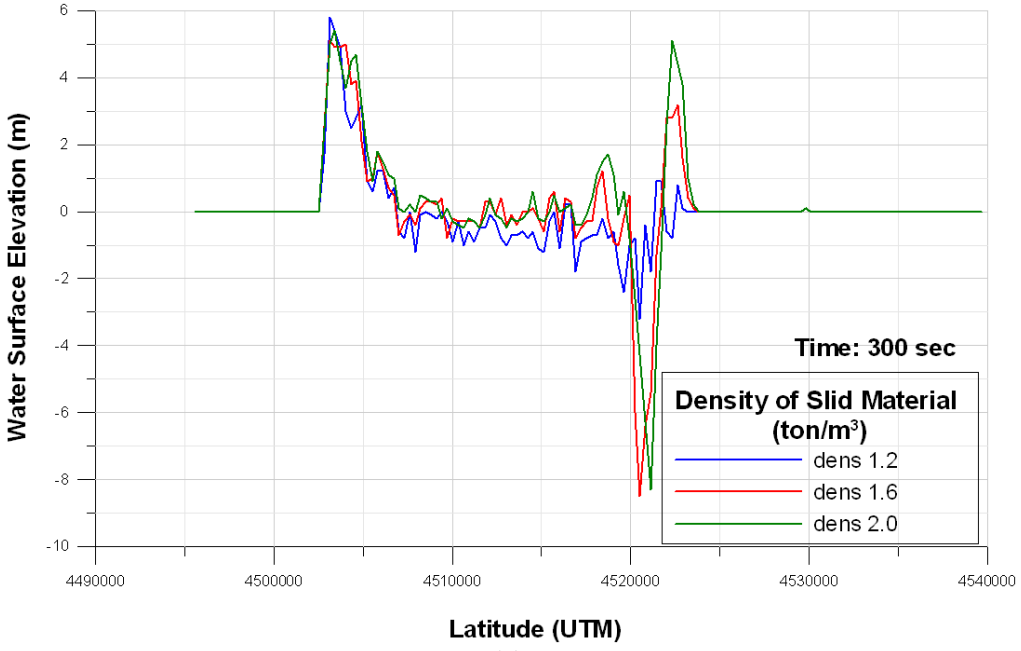

(e)

Figure 5.10: The Sea State along the Cross Section at Time 60 (a), 120 (b), 180 (c), 240 (d), and 300 (e) Seconds for 3 Selected Density Values

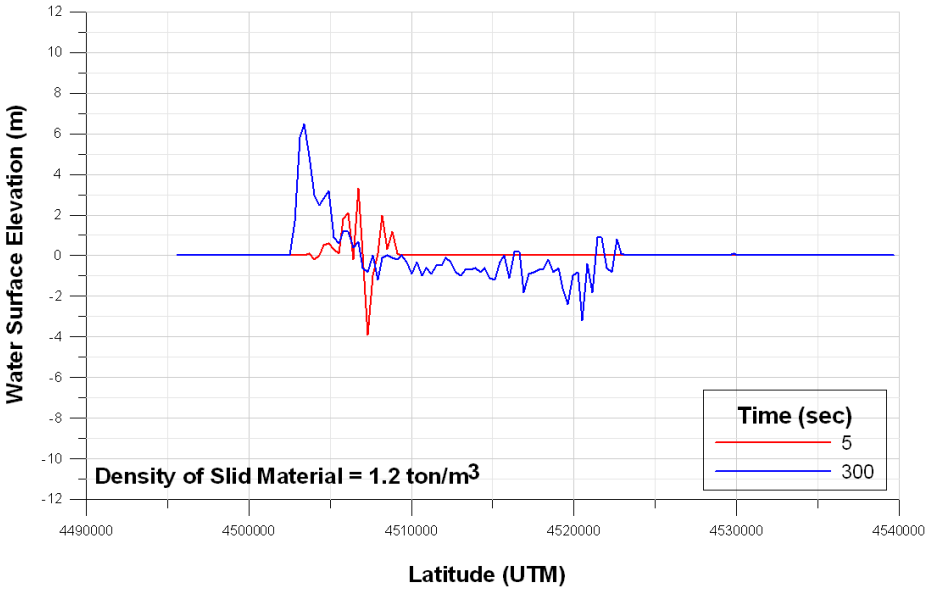
Water Surface Elevation (m)
12
10
8
6
4
2
0
-2
-4
-6
-8
-10
-12
Density of Slid Material = 1.2 ton/m3
Time (sec)
5
300
4490000
4500000
4510000
4520000
4530000
4540000
Latitude (UTM)

(a)

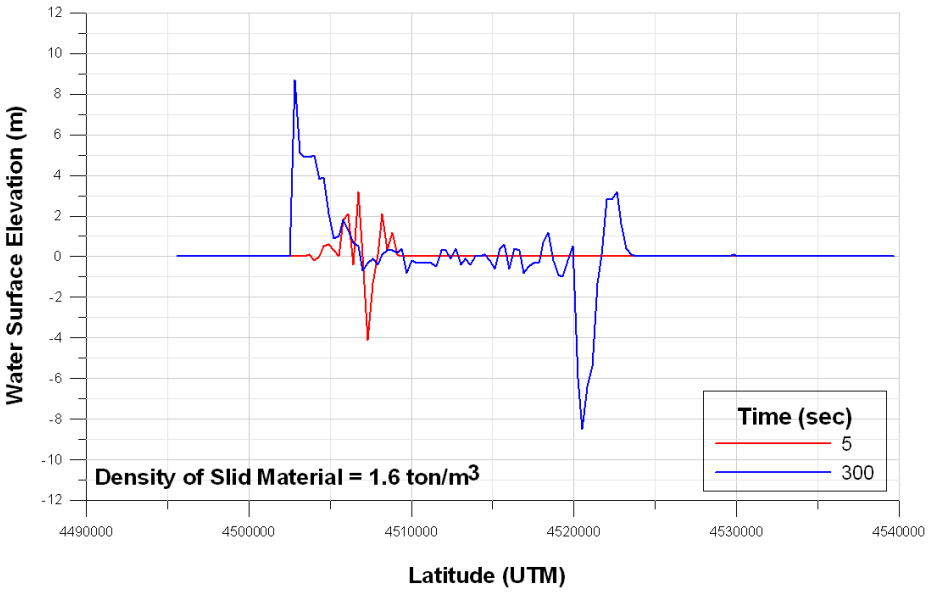
Water Surface Elevation (m)
12
10
8
6
4
2
0
-2
-4
-6
-8
-10
-12
Density of Slid Material = 1.6 ton/m3
Time (sec)
5
300
4490000
4500000
4510000
4520000
4530000
4540000
Latitude (UTM)

(b)

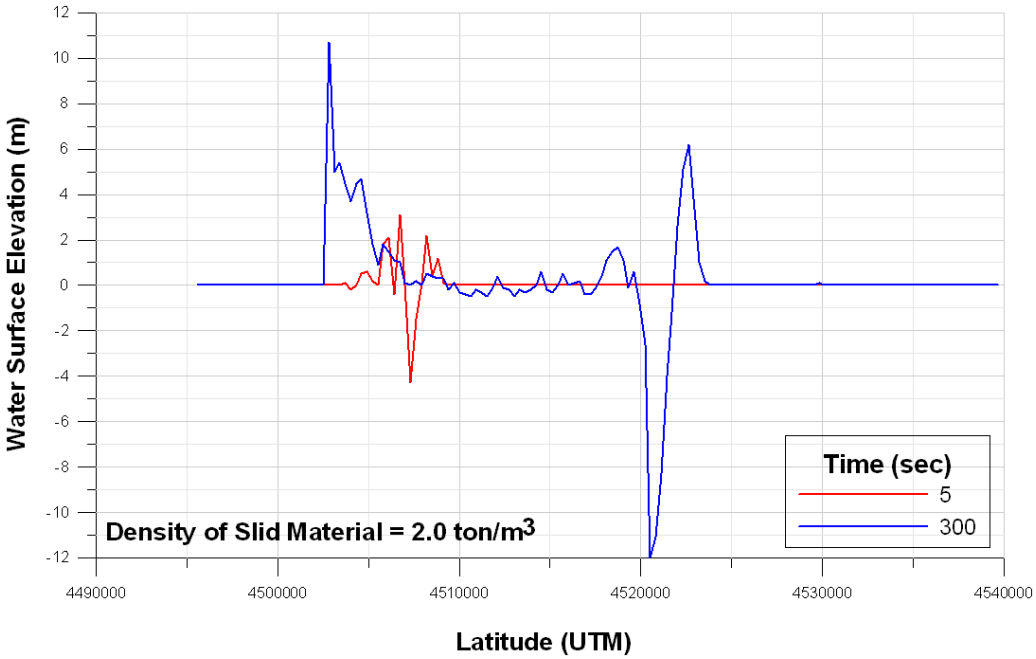

(c)

Figure 5.11: The Sea State Developed from the Tsunami Wave Generated by the Landslide, Which Has Mud Density of 1.2 (a), 1.6 (b) And 2.0 (c) ton/m^3 , at Different Times Accross the Cross Section.

Water surface along the cross section at 5 and 300 seconds (start and end of sliding) computed in the simulation are given in Figure 5.11 for the different densities (1.2, 1.6, 2.0 ton/m^3) of the slid material. Figure 5.11 shows that, the amplitude of the wave differs from each case. Higher density slid material cause higher amplitude surface elevation.

The maximum water elevations computed at every grid point during 5 minutes simulations are given in the Figure 5.12 for each density value. It is also seen that the propagation distance is similar but amplitudes are higher for high density slid material.

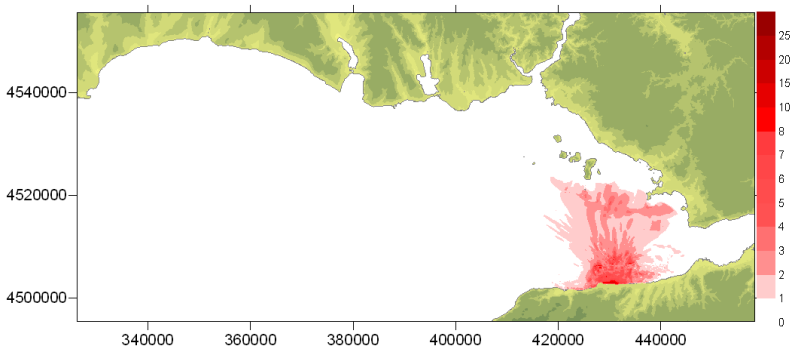

(a)

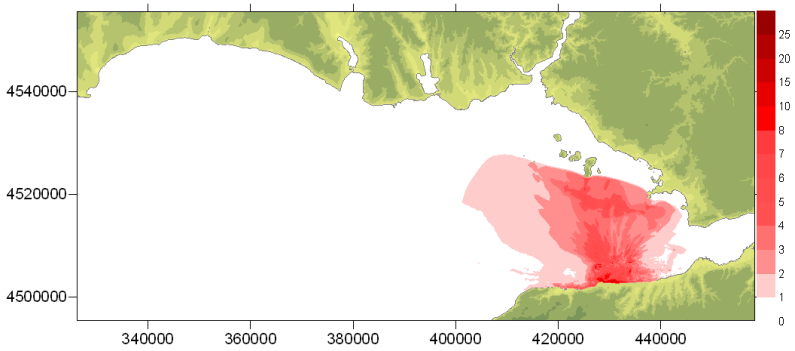

(b)

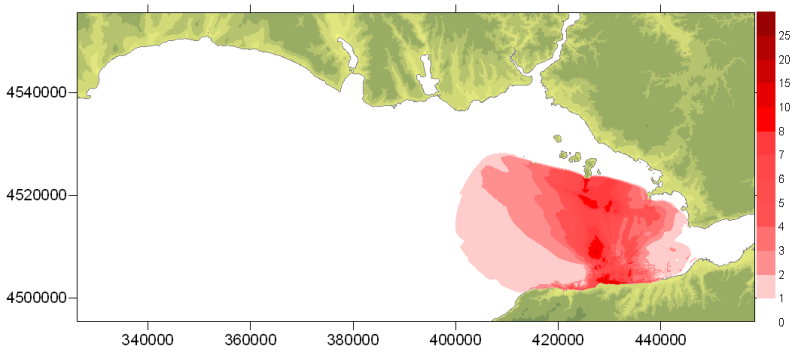

(c)

Figure 5.12: Maximum Water Elevation During 5 Minutes of Simulation of the Landslide Which Has Mud Density of 1.2 (a), 1.6 (b) and 2.0 (c) ton/m^3

The comparisons showing the change of the amplitude of the leading wave with respect to density of slid material and propagation time of the generated tsunami is given in Figures 5.13 and 5.14. It is seen from Figure 5.13 that the amplitude evolution is not dependent of the density of the slid material in first 2.5 minutes

duration. However, the linear relationship between amplitude and density is observed after 2.5 minutes of landslide. It is seen from Figure 5.14 that the evolution of the leading wave amplitude starts earlier if slid material is denser.

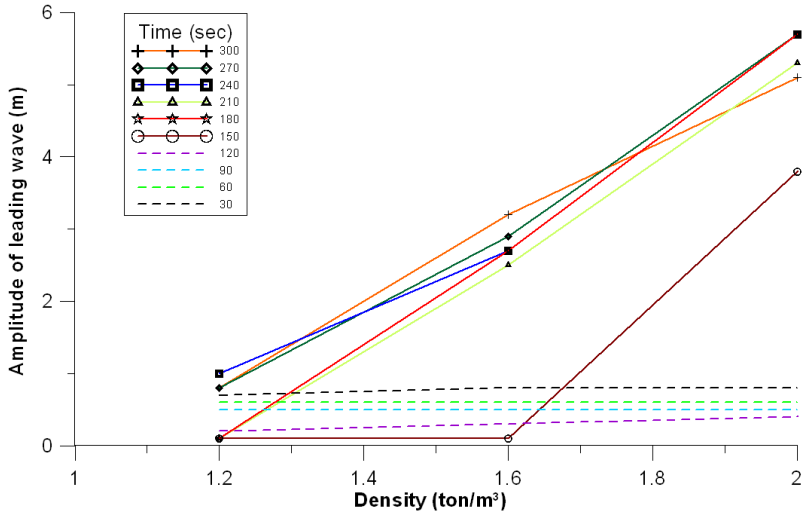

Figure 5.13: Amplitude of the Leading Wave vs. Density Graph at Different Time Steps

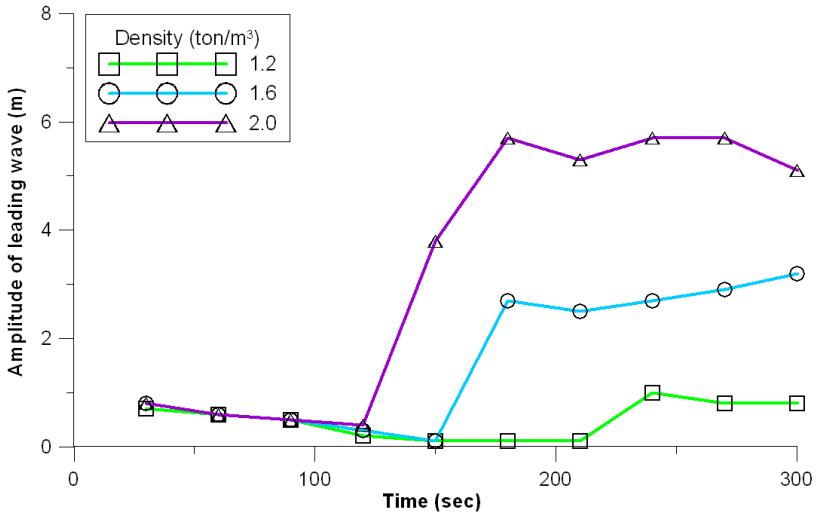

Figure 5.14: Amplitudes of the Leading Waves According to the Density of the Slid Material During 5 Minutes Simulation

5.2.2 Effect of thickness of of the slid material on tsunami generation

Thickness of the slid material is another parameter since the displaced mass of material cause more displacement of water and higher waves. A maximum thickness of 200m is assumed. the location of the slide and the thicknesses are patterned and digitized as Figure 5.15 in section 5.2. the total volume and area of this slide is calculated as 2.5 km^3 and 39 km^2, respectively. The cross section along south-north direction at landslide location in the Sea of Marmara is seen in Figure 5.16. The location of the slide is indicated on the Figure. The thickness of the maximum erosion and deposition in the slide is calculated as 110 m and 90 m, respectively (Figure 5.15). In order to investigate the slide thickness and amplitude of the leading wave, three different thicknesses of the slide is selected. They are i) the same thickness as in Figure 5.15 as thickness ratio (thickness constant) 1.0, ii) 20 % reduced thickness of the slide as thickness ratio 0.8, and iii) 50 % reduced thickness of the slide as thickness ratio 0.5. The cross sectional view of the wave propagation according to the slide thickness ratio (thickness constant) at different time steps are shown in the Figures 5.17 (a)-(e).

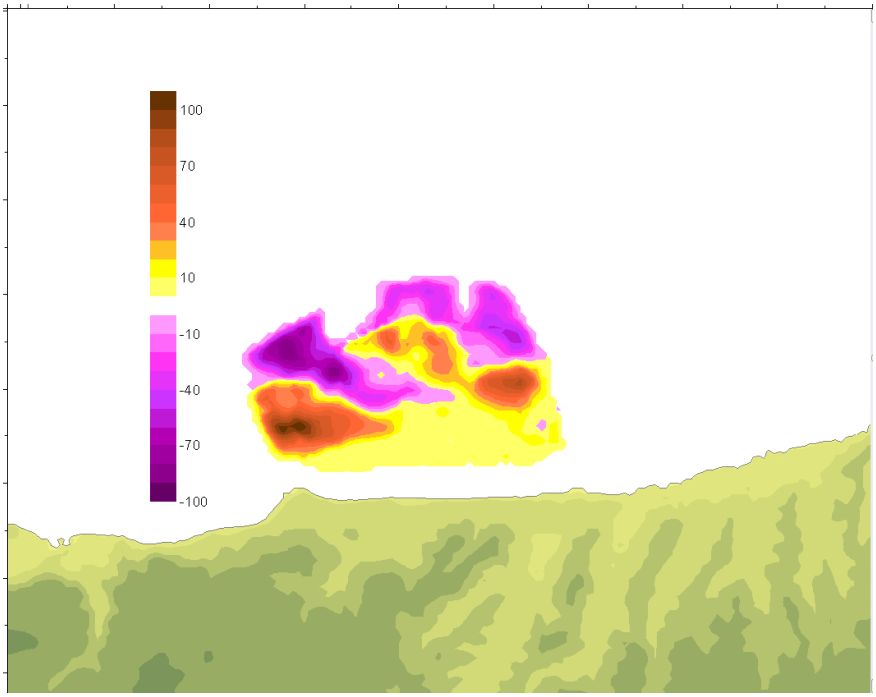

Figure 5.15: Digitized Slide Thickness Contours (Color Scale in Meters)

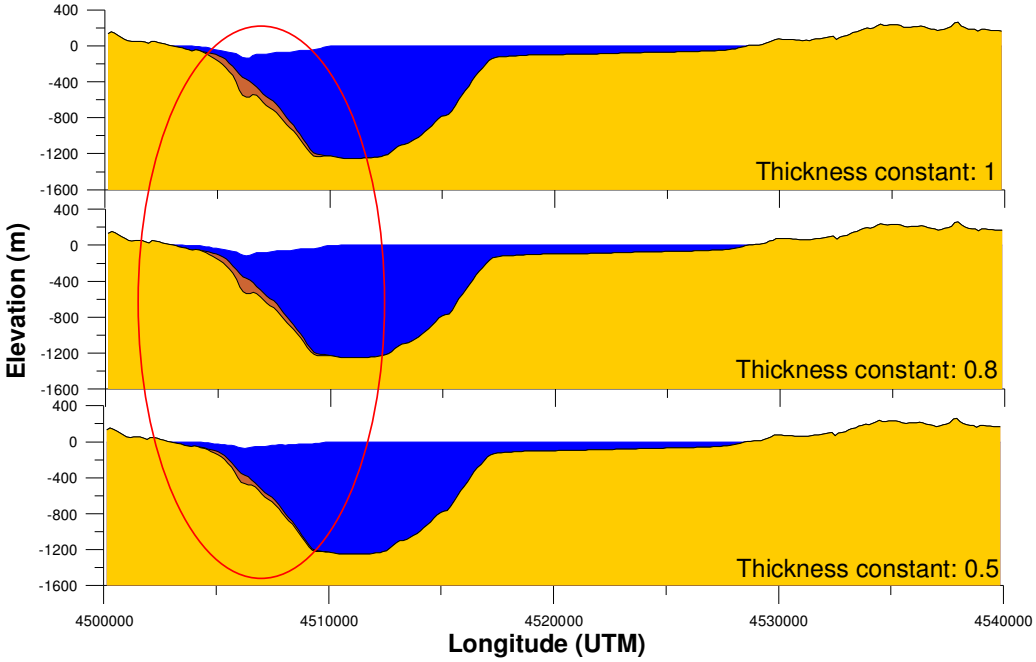

Figure 5.16: Schematization of the Different Sliding Mass Thicknesses

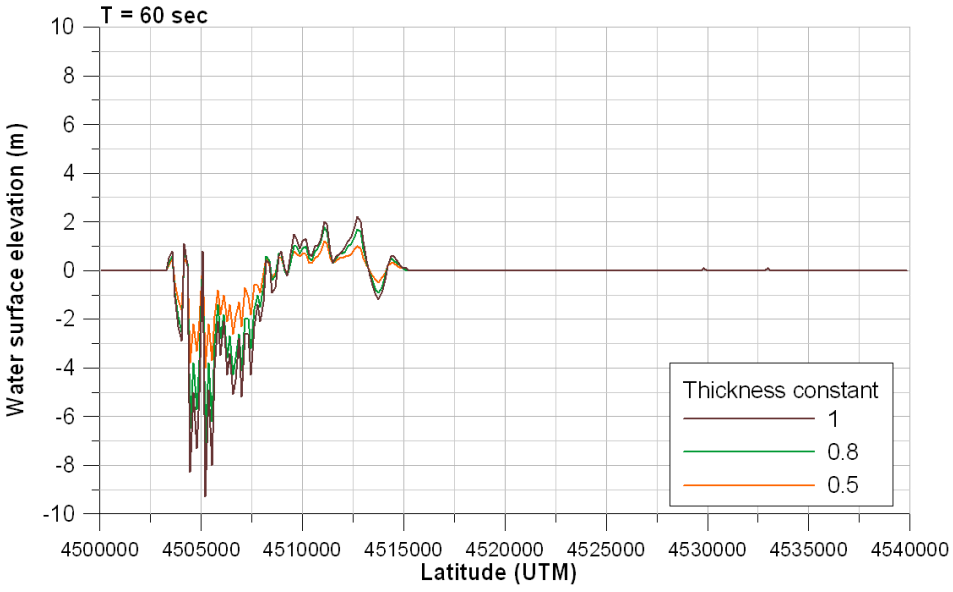

(a)

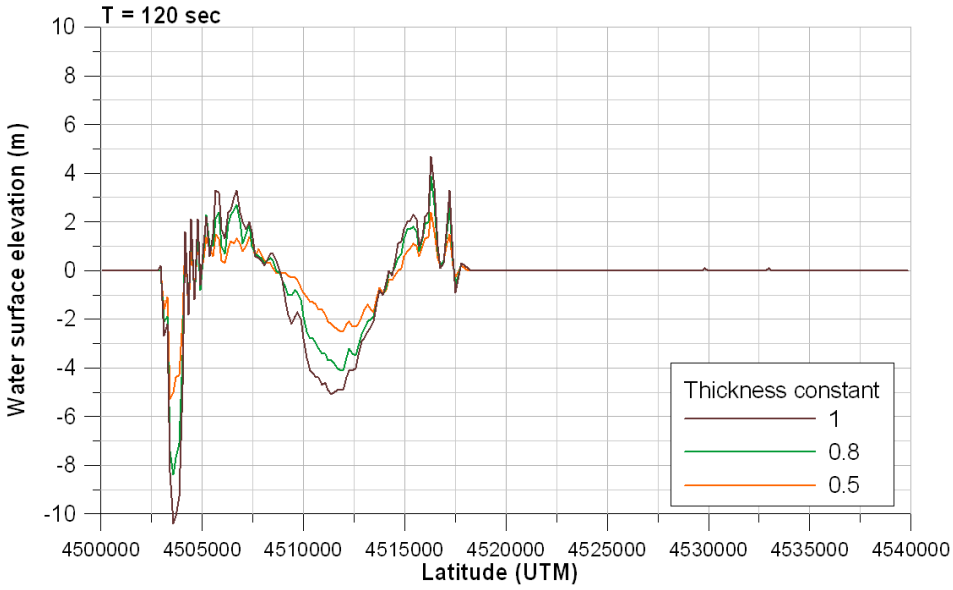
T = 120 sec
Water surface elevation (m)
10
8
6
4
2
0
-2
-4
-6
-8
-10
4500000
4505000
4510000
4515000
4520000
4525000
4530000
4535000
4540000
Latitude (UTM)
Thickness constant
1
0.8
0.5

(b)


T = 180 sec
Water surface elevation (m)
10
8
6
4
2
0
-2
-4
-6
-8
-10
4500000
4505000
4510000
4515000
4520000
4525000
4530000
4535000
4540000
Latitude (UTM)
Thickness constant
1
0.8
0.5

(c)

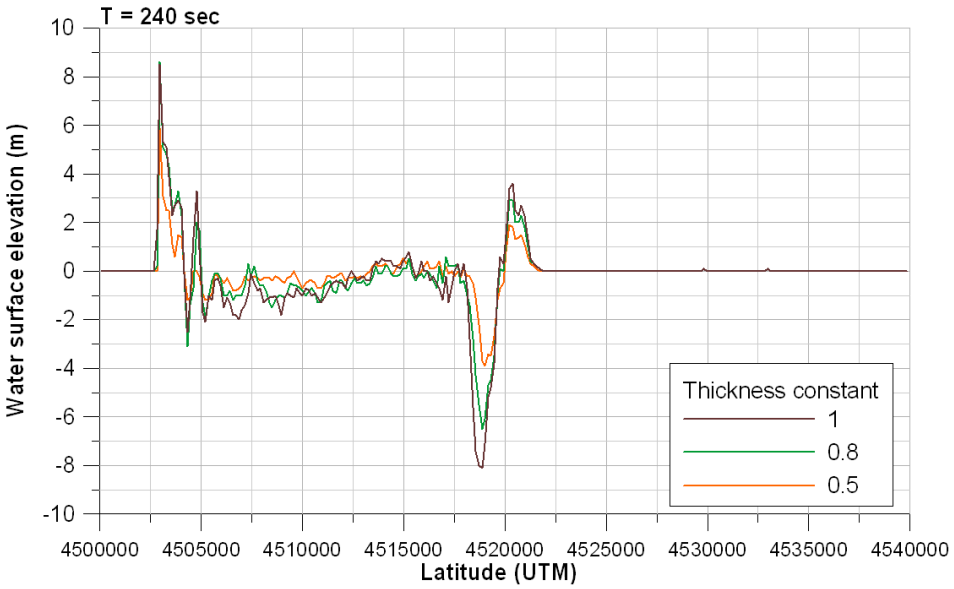

(d)

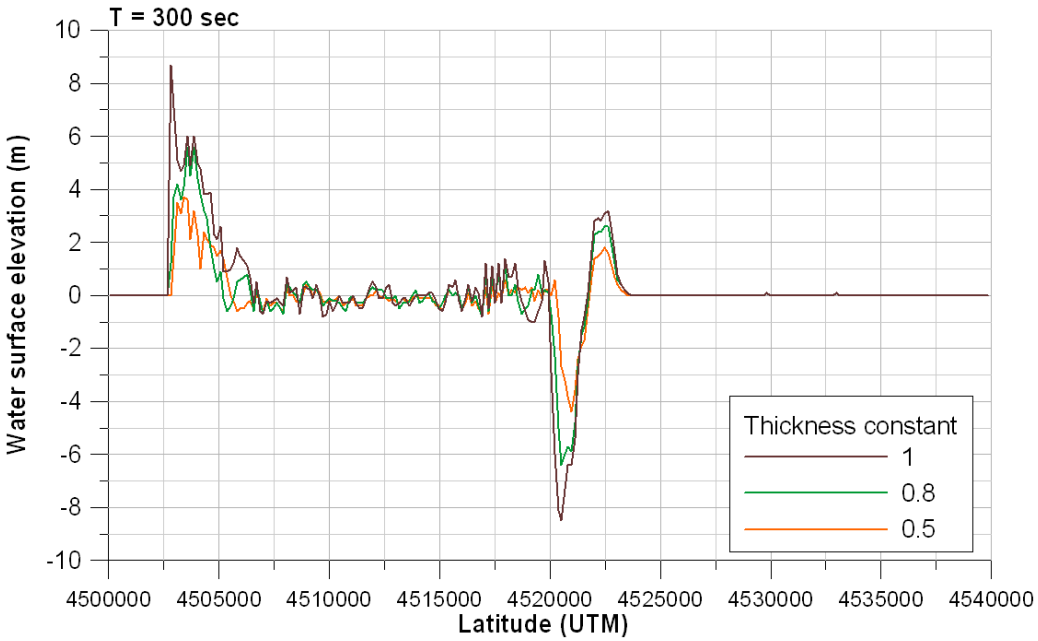

(e)

Figure 5.17: The Sea State Along the Cross Section for Different Landslide Thickness Constants at Times 1 (a), 2 (b), 3 (c), 4 (d) and 5 (e) Minutes

It can be seen from the Figure 5.18 that the relation between leading wave amplitude and slide thickness ratio can be considered as linear in the range of data used in the study.

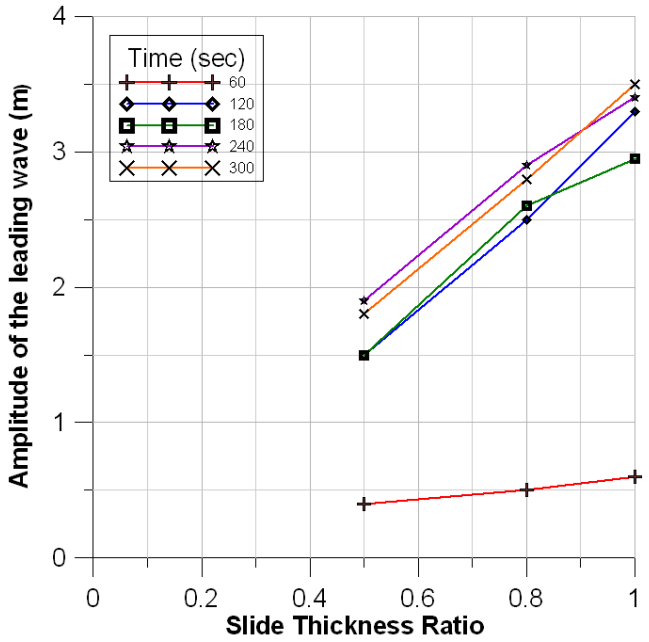

Figure 5.18: Relation Between Leading Wave Amplitude and Slide Thickness Ratio at Different Time Steps

In the next chapter, the propagation of the landslide induced tsunami waves is investigated by choosing an appropriate mud density and slide thickness.

CHAPTER 6

PROPAGATION AND COASTAL EFFECTS AT OFFSHORE YALOVA

In this chapter, the propagation of the tsunami wave induced by Offshore Yalova (ON1) landslide and its effects on northeast part of Sea of Marmara coasts are observed. During the simulation the density of the sliding mud is taken as 1.6 ton/m^3 while maximum thickness of the slide is taken as 200m.

After 5 minutes of simulation of the landslide generated tsunami with TWO LAYER model, the propagation of the tsunami waves is simulated with NAMI-DANCE. NAMI DANCE is developed for tsunami numerical modeling in collaboration with Ocean Engineering Research Center, Middle East Technical University, Turkey and Department of Nonlinear Geophysical Institute of Applied Physics, Russian Academy of Science, Russia using the identical computational procedures of TUNAMI N2. Developing the model TUNAMI N2 has been the most important development in tsunami modeling achieved by Profs. Shuto and Imamura. TUNAMI N2 determines the tsunami source characteristics from earthquake rupture characteristics. It computes all necessary parameters of tsunami behavior in shallow water and in the inundation zone allowing for a better understanding of the effect of tsunamis according to bathymetric and topographical conditions (Imamura, 1989, Shuto, Goto, Imamura, 1990, Goto and Ogawa, 1991). Like TUNAMI N2, NAMI DANCE is based on the solution of nonlinear form of the long wave equations with respect to related initial and boundary conditions. In general, the explicit numerical solution of Nonlinear Shallow Water (NSW) Equations is preferable for the use since it uses reasonable computer time and memory, and also provides the results in acceptable error limit.

For input, the 150 m grid sized bathymetry, gauge point locations, the sea state after 5 minutes from the starting of the slide water discharge files are inserted to the model.

Along the northeast coast of the Sea of Marmara, 22 synthetic gauge points are selected which are shown in Figure 6.1 and the coordinates and depths of these points are given in Table 6.1.

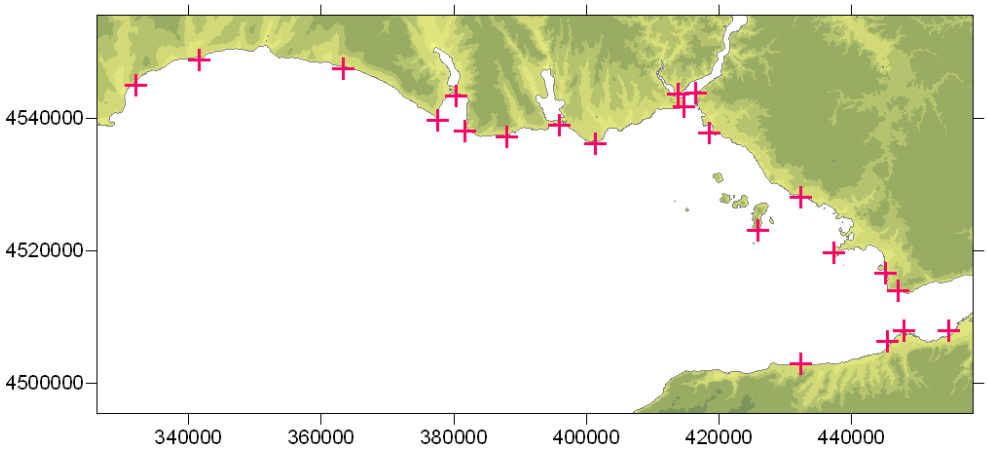

Figure 6.1: Gauge Point Locations

The sea states at different time steps are plotted in Figures 6.2. According to the simulation results, it can be observed that the tsunami wave reaches Yalova and Çınarcık coasts in less than 5 minutes Prince Islands (Büyükada) in 5 minutes, and Istanbul coasts in 15 minutes. As for northwest part of the study domain (Silivri, Küçükçekmece, Büyükçekmece), Silivri coasts, the wave reaches the area nearly in half an hour.

Table 6.1: Gauge Point Coordinates and Depths

Name	X coordinate (UTM)	Y coordinate (UTM)	Depth (m)
Silivri 1	332086.025	4545033.7875	8.4
Silivri 2	341540.75	4548788.50625	9.4
Silivri 3	363301.625	4547436.8075	8.1
Büyükçekmece 1	377558.75	4539777.18125	10.1
Büyükçekmece 2	380410.175	4543381.71125	5.7
Büyükçekmece 3	381610.775	4538125.105	7.6
Ambarlı Limanı	388064	4537223.9725	8.7
Küçükçekmece	395867.9	4539026.2375	5.6
Yeşilköy	401420.675	4536172.65125	9.0
Sultanahmet	414777.35	4541729.635	18.2
Haliç girişi	413876.9	4543682.08875	14.6
Üsküdar	416428.175	4543832.2775	-9.2
Fenerbahçe	418529.225	4537824.7275	-2.5
Büyükada	425882.9	4523106.23	35.2
Tuzla	437288.6	4519651.88875	-1.5
Gebze 1	445092.5	4516648.11375	4.5
Gebze 2	447043.475	4513944.71625	22.9
Yalova 1	447943.925	4507937.16625	1.6
Yalova 2	454697.3	4507937.16625	3.6
Yalova 3	445392.65	4506285.09	4.1
Çınarcık	432336.125	4502980.9375	1.0
Pendik	432336.125	4528060	11.8

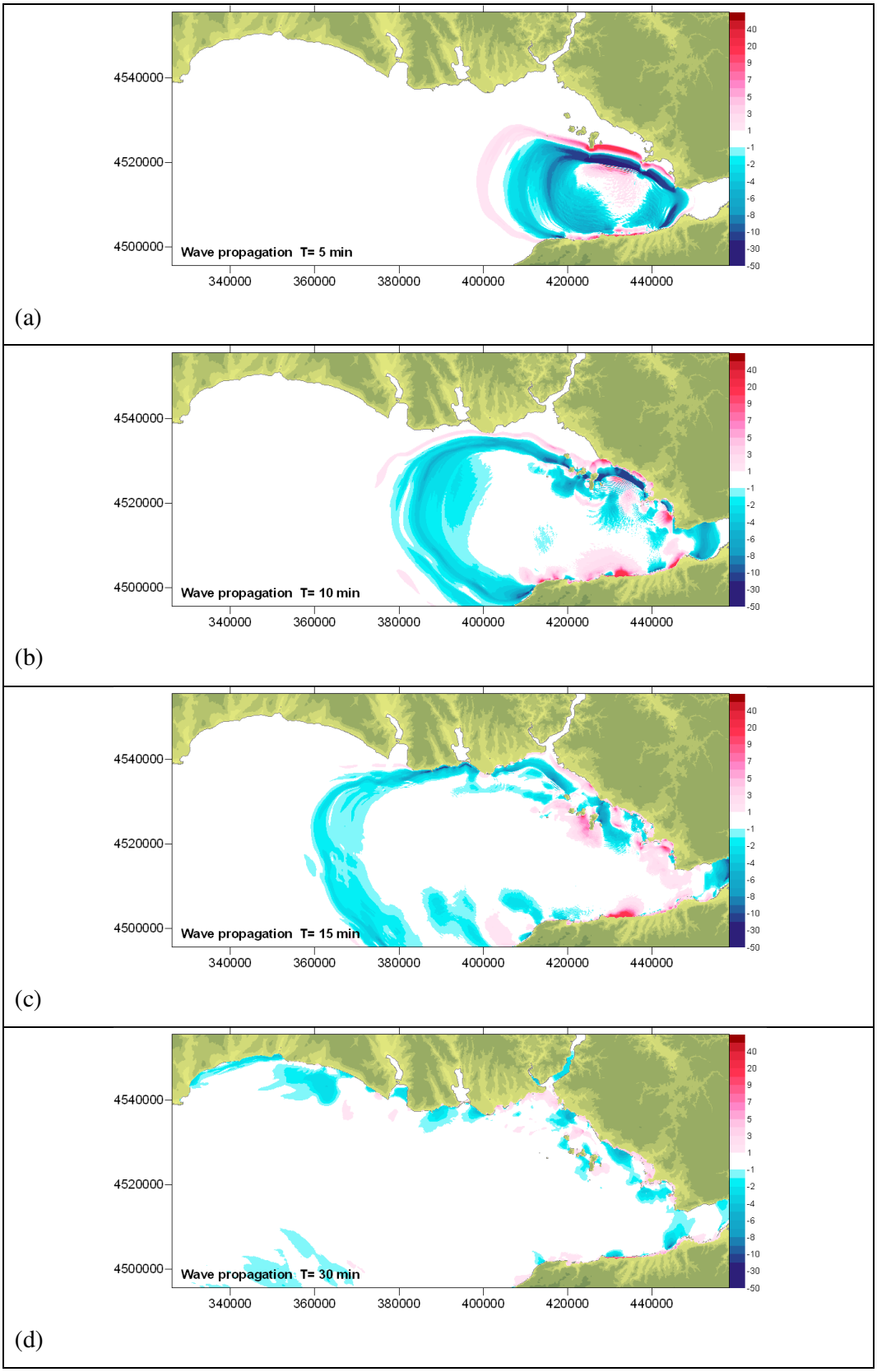

Figure 6.2: The Sea States At Different Time Steps

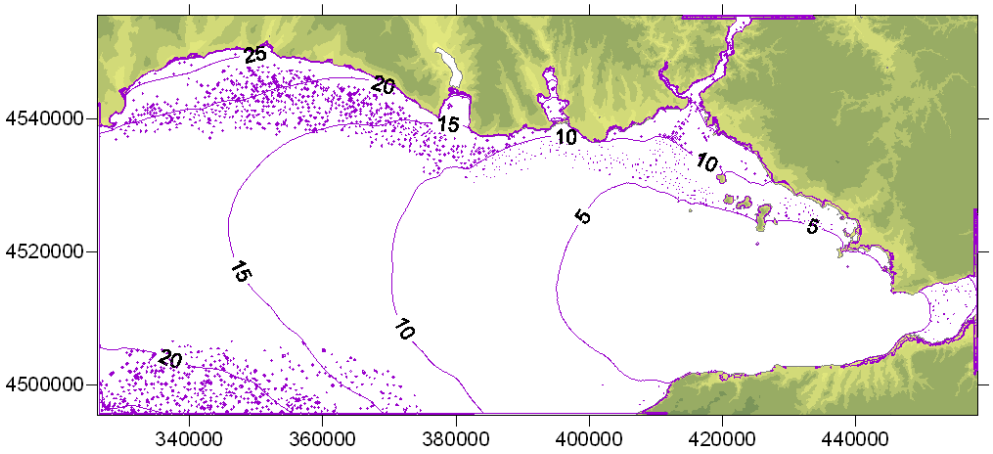

Figure 6.3: Arrival Time of First Wave in Minutes

The maximum water elevation is 18.4m and shown in Figure 6.6. As it can be seen from the figure, the most affected areas affected by the landslide are the south and north coast along the location the slide occurs. Prince Islands prevent harsher damage along Istanbul coasts, yet Buyukada coasts are highly affected by the wave induced by ON1 landslide.

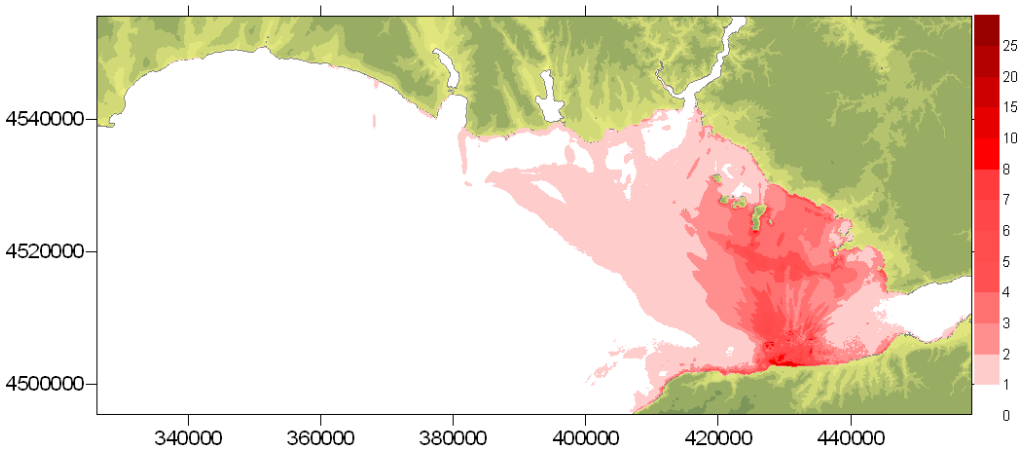

Figure 6.4: Maximum Water Elevation (m)

The time histories of selected gauge points are shown in Figure 6.5 (a) to (m)

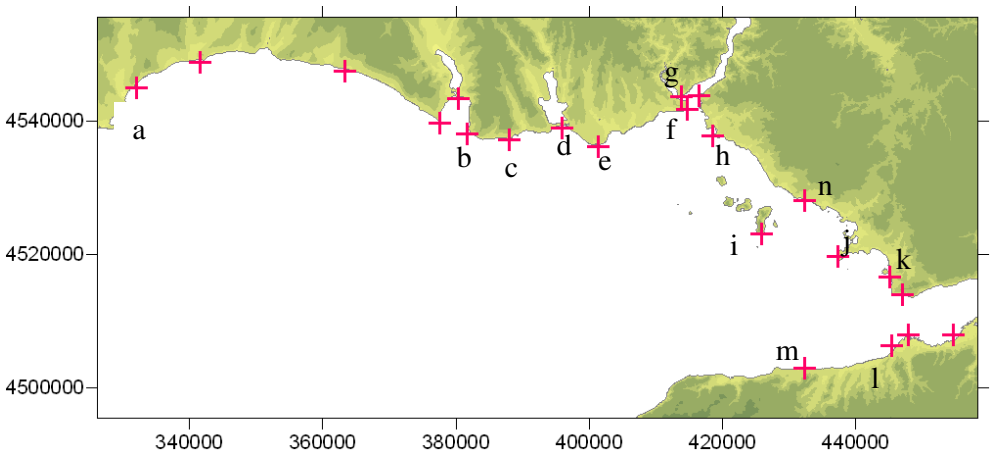

Figure 6.5: Selected gauge points, the time histories of these points are shown in Figure 6.6 (a) to (n)

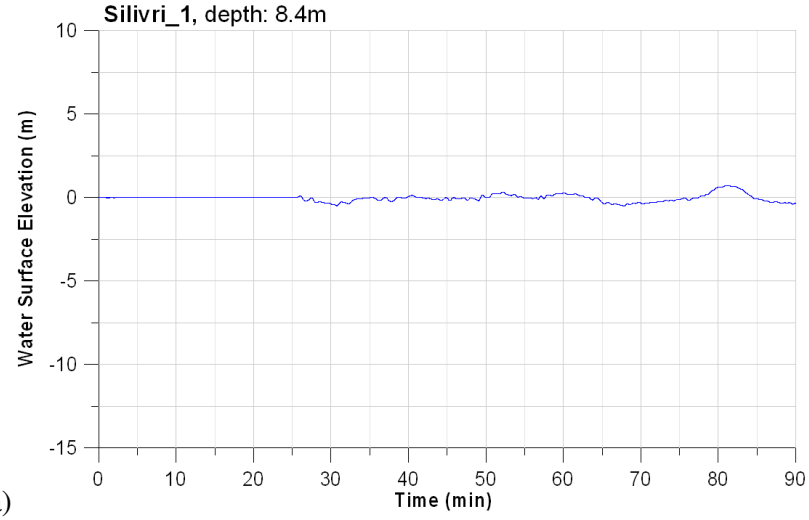

(a)

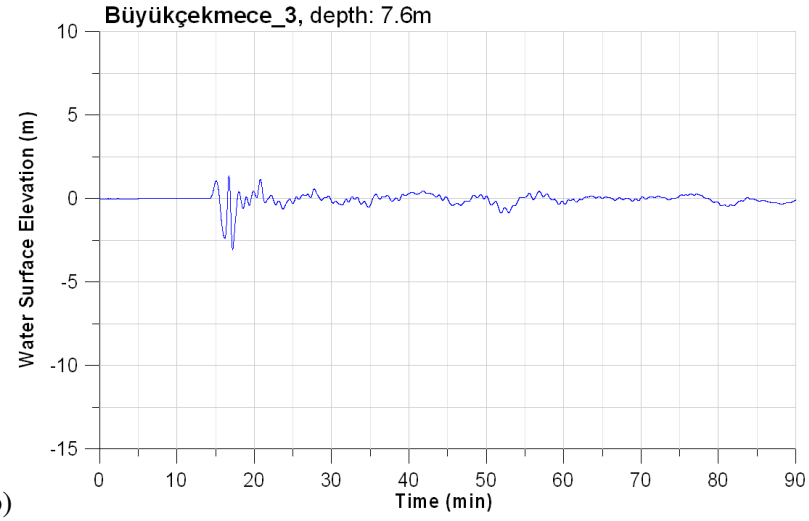
Büyükçekmece_3, depth: 7.6m
Water Surface Elevation (m)
10
5
0
-5
-10
-15
0
10
20
30
40
50
60
70
80
90
Time (min)

(b)

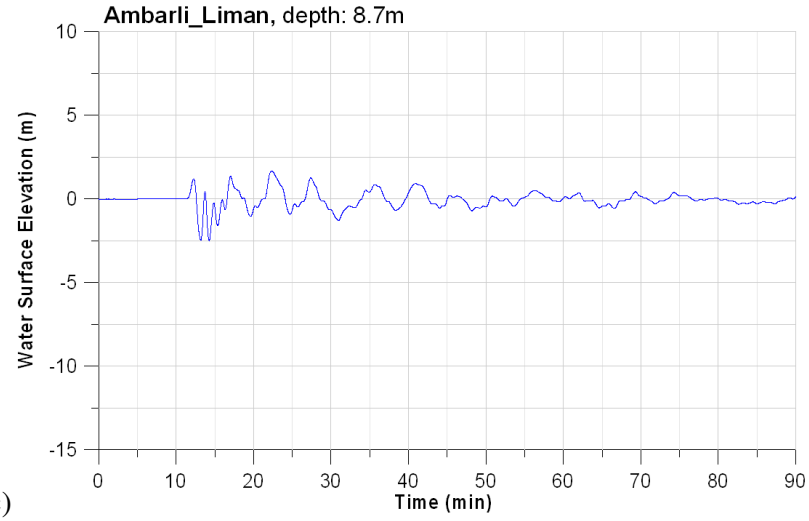
Ambarli_Liman, depth: 8.7m
Water Surface Elevation (m)
10
5
0
-5
-10
-15
0
10
20
30
40
50
60
70
80
90
Time (min)

(c)

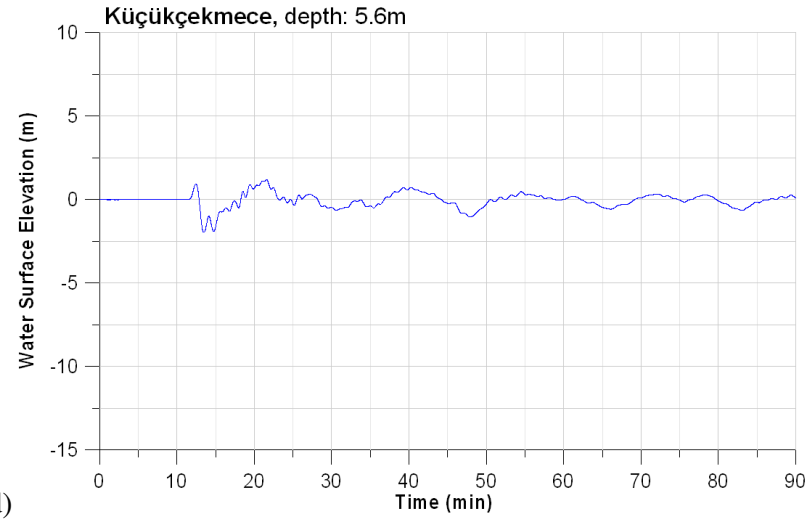
Küçükçekmece, depth: 5.6m
Water Surface Elevation (m)
10
5
0
-5
-10
-15
0
10
20
30
40
50
60
70
80
90
Time (min)

(d)


Yesilköy, depth: 9m
Water Surface Elevation (m)
10
5
0
-5
-10
-15
0
10
20
30
40
50
60
70
80
90
Time (min)

(e)

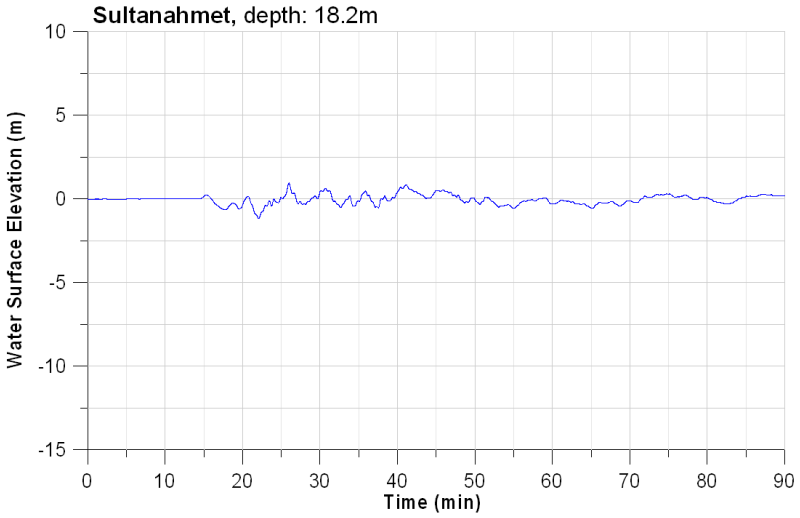
Sultanahmet, depth: 18.2m
Water Surface Elevation (m)
10
5
0
-5
-10
-15
0
10
20
30
40
50
60
70
80
90
Time (min)

(f)

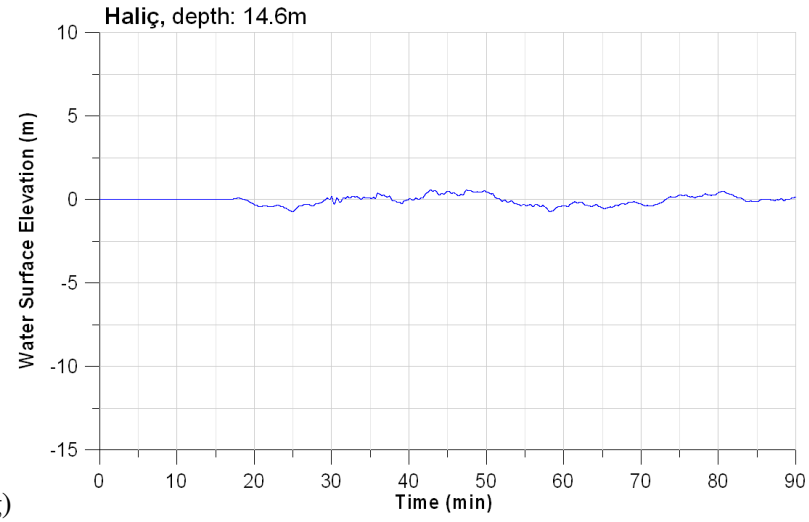
Haliç, depth: 14.6m
Water Surface Elevation (m)
10
5
0
-5
-10
-15
0
10
20
30
40
50
60
70
80
90
Time (min)

(g)

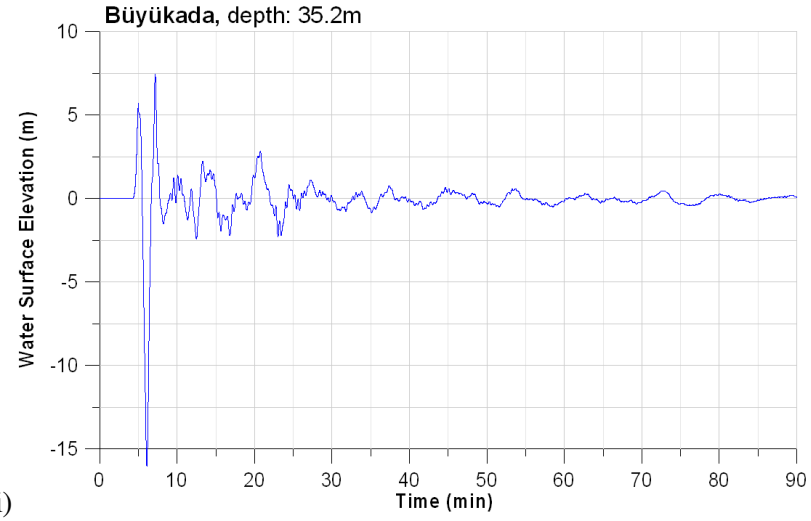
Büyükada, depth: 35.2m
Water Surface Elevation (m)
Time (min)

(i)

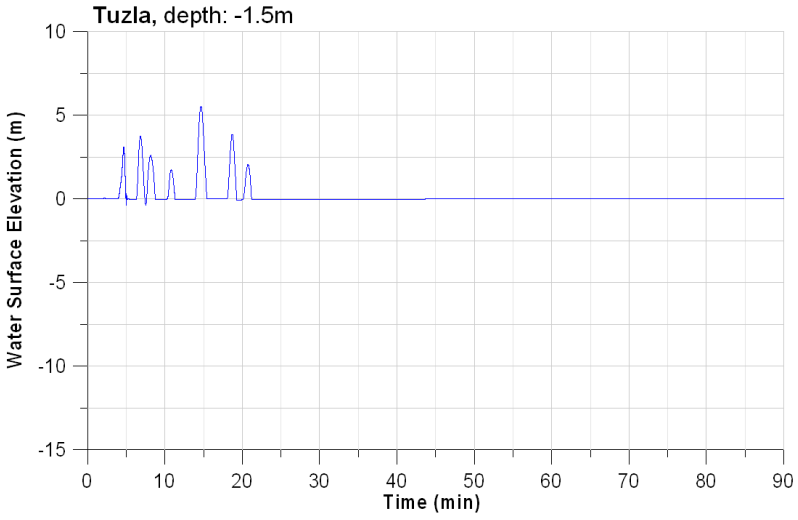
Tuzla, depth: -1.5m
Water Surface Elevation (m)
Time (min)

(j)

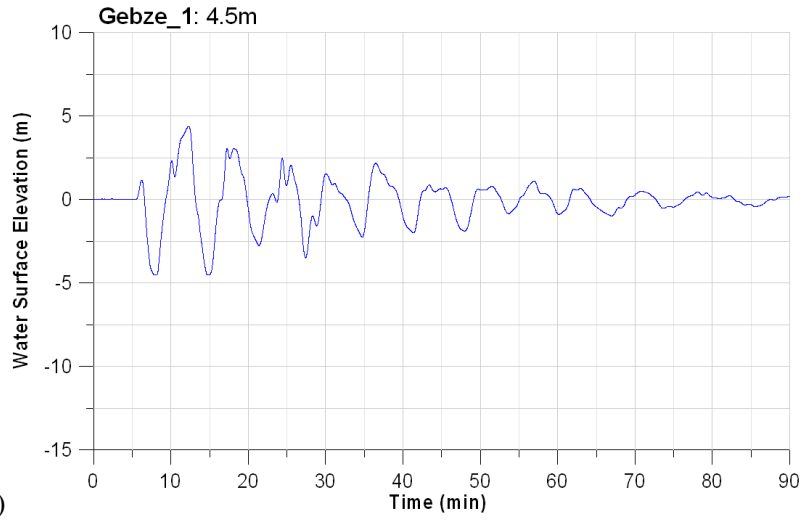
Gebze_1: 4.5m
Water Surface Elevation (m)
Time (min)

(k)

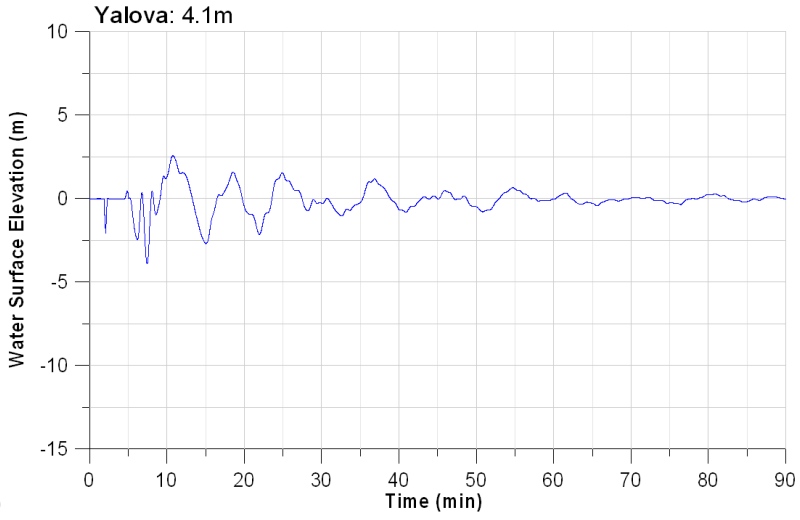

(l)

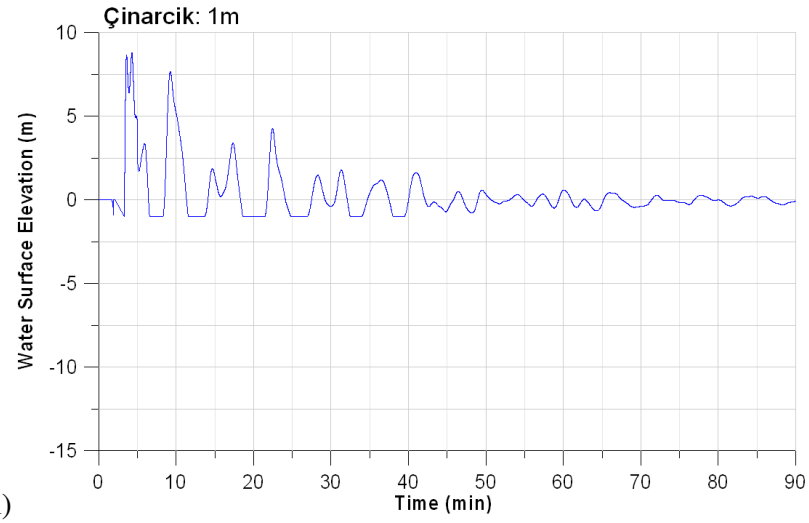

(m)

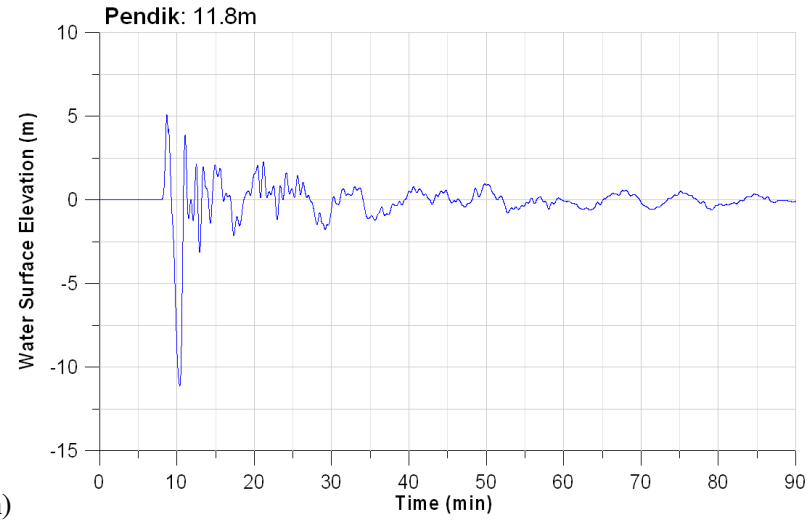

(n)

Figure 6.6: The Time Histories of Selected Gauge Points

The depths, arrival times of first waves, arrival times of maximum waves, maximum and minimum water elevation amplitudes for the 22 selected gauge points are summarized in Table 6.2. According to the table, Büyükada, Gebze, Çınarcık and Pendik regions are in danger.

Table 6.2: Summary of results of the selected case

Gauge Point	***Depth (m)***	***T_first (min)***	***T_max (min)***	***Amplitude (+) (m)***	***Amplitude (-) (m)***
Silivri1	8.4	26	81	0.7	-0.5
Silivri2	9.4	27	49	0.7	-0.7
Silivri3	8.1	22	38	0.9	-1.1
Buyukcekmece1	10.1	16	20	0.7	-1.6
Buyukcekmece2	5.7	21	36	0.7	-1.4
Buyukcekmece3	7.6	15	17	1.4	-3.0
Ambarli_Liman	8.7	12	22	1.7	-2.5
Kucukcekmece	5.6	13	22	1.2	-2.0
Yesilkoy	9	10	10	1.4	-2.8
Sultanahmet	18.2	15	26	1.0	-1.2
Halic	14.6	19	43	0.6	-0.7
Buyukada	35.2	< 5	7	7.6	-16.0
Tuzla	-1.5	< 5	15	5.6	-0.4
Gebze1	4.5	6	12	4.4	-4.5
Gebze2	22.9	< 5	14	1.4	-2.3
Yalova1	1.6	6	11	1.7	-1.5
Yalova2	3.6	10	17	1.7	-2.4
Yalova3	4.1	< 5	11	2.6	-3.9
Cinarcik	1	< 5	9	8.7	-1.0
Pendik	11.8	8	9	5.1	-11.1

The distributions of maximum surface elevation that the waves cause near the shoreline along north and south coasts in the Sea of Marmara are shown in Figure 6.7. According to the figure, the maximum positive amplitude of the water surface near the shoreline up to 20 m water depth values exceed 7m at the north shore and 18.5m at the south coast near landslide location, which are surprisingly high values for the Sea of Marmara. The reason of such high values is probably because of that, during the simulation, the landslide is estimated including the portion of the past landslide eroded mass of "OR1894".

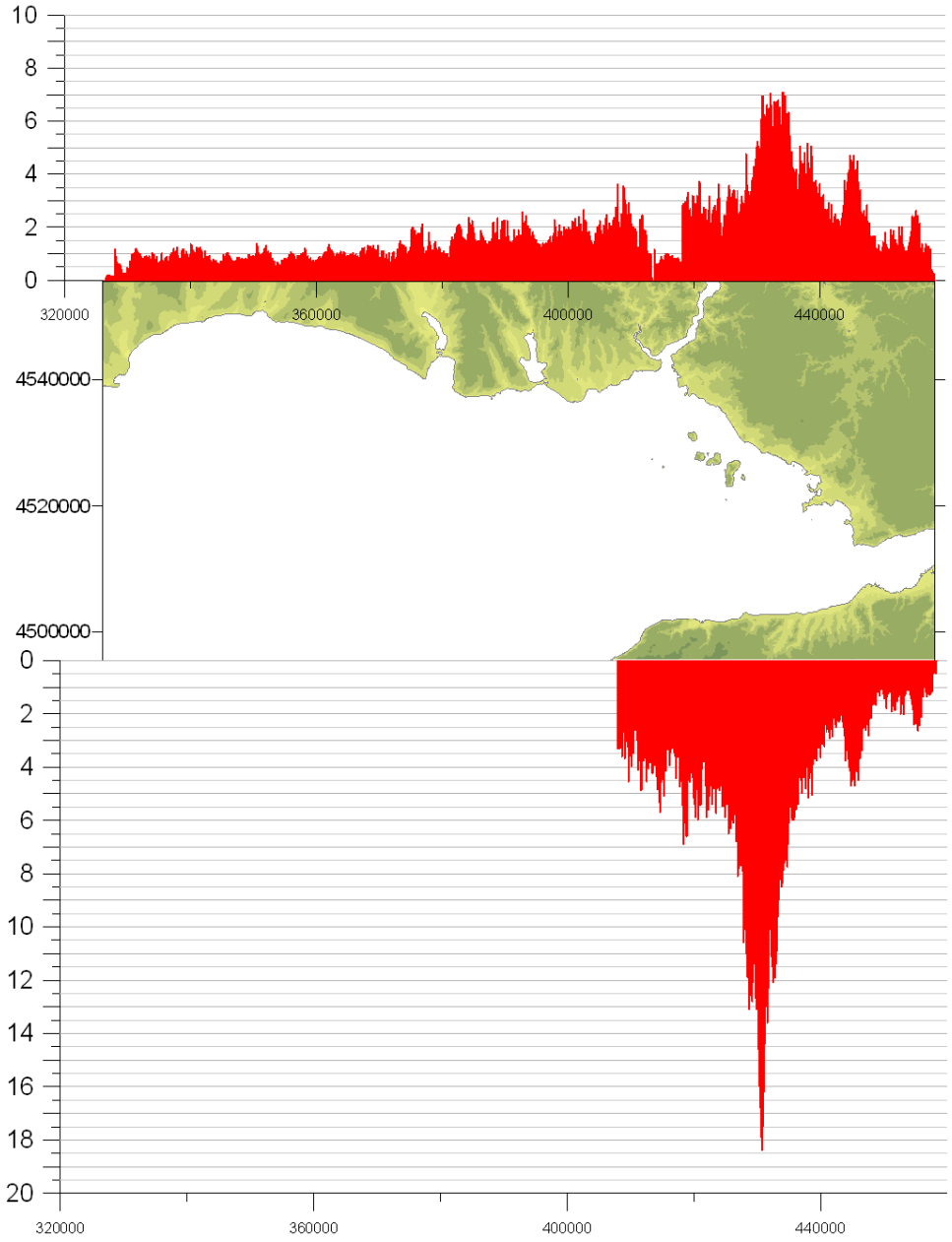

Figure 6.7: Maximum Water Level Distributions (m) along North and South Coasts of Marmara within 90 Minutes Simulation

CHAPTER 7

DISCUSSIONS AND CONCLUSIONS

In this thesis, the complex phenomena: landslide generated tsunamis, are studied. The generation mechanism and controlling parameters of this phenomenon are investigated. The information about the landslide generated tsunami events occurred in history are gathered and summarized. The landslide parameters (volume of slide, thickness of the slid material, characteristic speed with which the slide moves (or total distance moved by the slide and duration of the slide), acceleration, depth of water above slide, angle of the slide from the horizontal (or vertical) direction, density of the slide material, coherent nature of the slide and grain size.) affecting the amplitude of the tsunami source are discussed. Among these parameters, the effects of the *density* and *thickness* of the slid material on the tsunami wave height is investigated by using the simulation code TWO-LAYER. In order to understand the effects of these two parameters, one of the probable landslides (at offshore Yalova) in the Sea of Marmara is selected as a case study. The main reasons of choosing the Sea of Marmara as the case study are; i) there are active fault zones in the region, ii) there is quite satisfactory bathymetric data and iii) the highly utilized and densely populated coastal areas in the region.

In order to analyze the effects of density of the slid material to the generated tsunami wave height, three different densities (1.2, 1.6, 2.0 ton/m^3) are simulated with thickness and volume of the landslide being constant. The analyses showed that the higher density of the slide material caused higher surface elevation waves. The comparisons showing the change of the amplitude of the leading wave with respect to density of slid material and propagation time of the generated tsunami showed that the amplitude evolution is not dependent of the density of the slid material in first 2.5 minutes duration. However, the linear relationship between amplitude and density is

observed after 2.5 minutes of landslide. Also, the evolution of the leading wave amplitude starts earlier if slid material is denser.

Secondly, the effects of thickness of the slid material to the generated tsunami wave height, three different thicknesses are simulated using the density of the landslide as constant. A maximum thickness of 200m for an irregular shape of landslide is assumed using Oyo and IMM, (2007). In order to investigate the effect of the landslide thickness on the amplitude of the wave, three different thicknesses of the landslide material are selected in the relative order of 1.0, 0.8 and 0.5. The results showed that higher thickness values cause higher water surface elevations (wave amplitudes) and the relation between leading wave amplitude and slide thickness ratio can be considered as linear in the range of data used in the study.

After analysing the effects of density and thickness of the slid material, appropriate values for density and thickness is selected. As a case study (landslide occurence at offshore Yalova; case name ON1), the density of slid material is selected as 1.6 ton/m^3 and maximum thickness of the landslide material is selected as 200m. In final part of the study, by using this data and the landslide volumes (before and after the slide) given in Oyo and IMM, (2007), the propagation and coastal amplification of the landslide generated tsunamis in the Sea of Marmara are simulated. During 90 minutes simulation, the maximum elevations at every grid in the study domain, the time histories at selected gauge locations, arrival times of the first and maximum waves are computed and presented graphically. According to the simulation results, it is observed that the tsunami waves (generated by the landslide at offshore Yalova) reaches Yalova and Çınarcık coasts in less than 5 minutes, Prince Islands (Büyükada) in 5 minutes, and Istanbul coasts in 15 minutes. As for northwest part (west coast of Istanbul) of the study domain (Silivri, Küçükçekmece, Büyükçekmece), Silivri coasts, the wave reaches the area nearly in half an hour. The maximum water elevations are in the order of 7 meters for northern coasts of Marmara Sea and 18.5m for southern coasts. These results are also compatible with the OYO and IMM, (2007) (See also Figure 7.1). The reason of the difference between OYO and IMM (2007) and the results in this study are the difference between the landslide motion used in both studies.

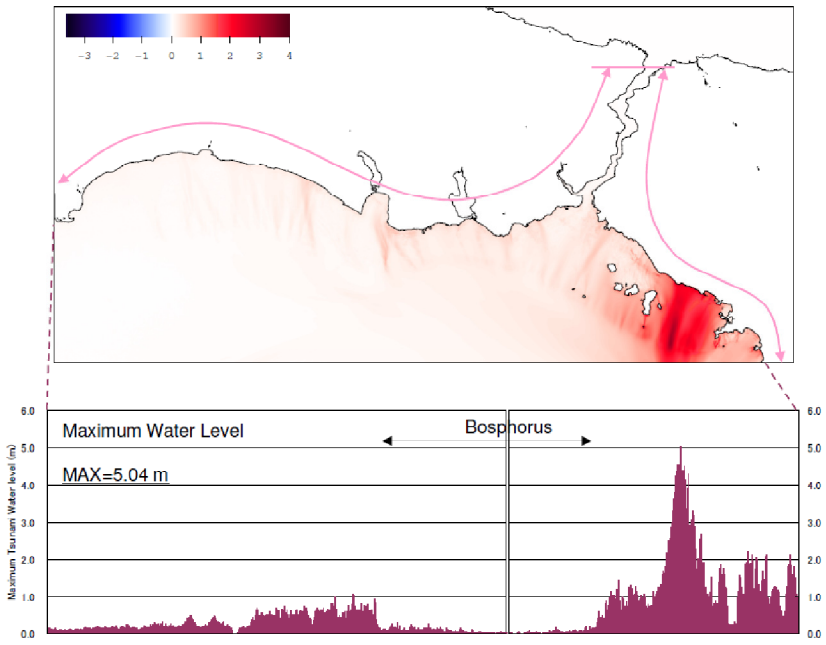

Figure 7.1: Maximum Water level and Inundation depth after 50 m grid simulation (OYO and IMM, 2007)

As an additional academic study, the tsunami generation by the full volume of the landslide material at offshore Yalova is also simulated and the results are discussed. It is found that if the full volume of landslide (2.9 km^3) at offshore Yalova slid that the wave amplitudes near the coastal areas becomes extremely high. Figure 7.2 shows that in the extreme case the maximum water level can increase to 38.6 m which is 20 meters higher that the original case. Also, comparing the water surface elevations for gauge point Pendik, for ON1 normal case (0.5 km^3 slide volume) and extreme case (2.5 km^3 slide volume) it can be seen from Figure 7.3 that the wave height in the extreme case is much higher.

In order to analyze the relation between wave evolution and thickness/volume of the landslide, further study is necessary using regular shaped basin with a uniform inclined slope.

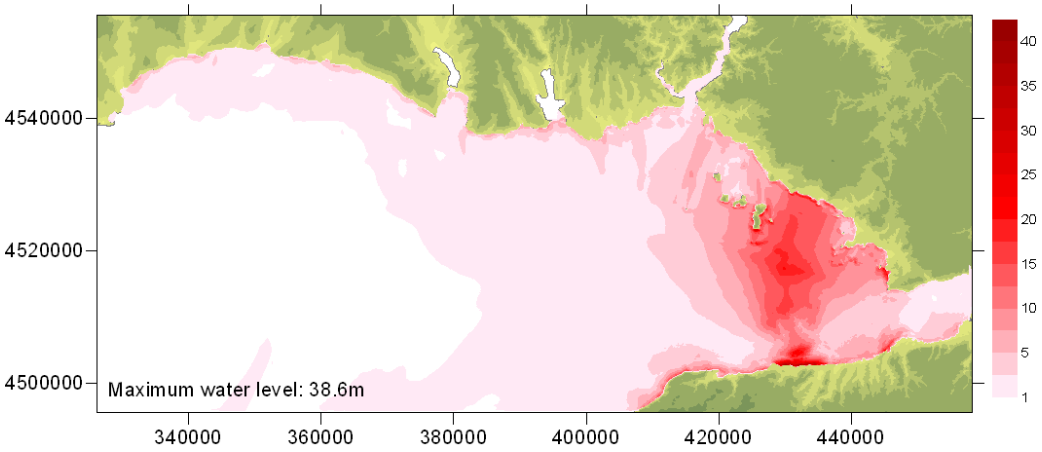

Figure 7.2: Maximum Water Elevation (m) as a result of the extreme case

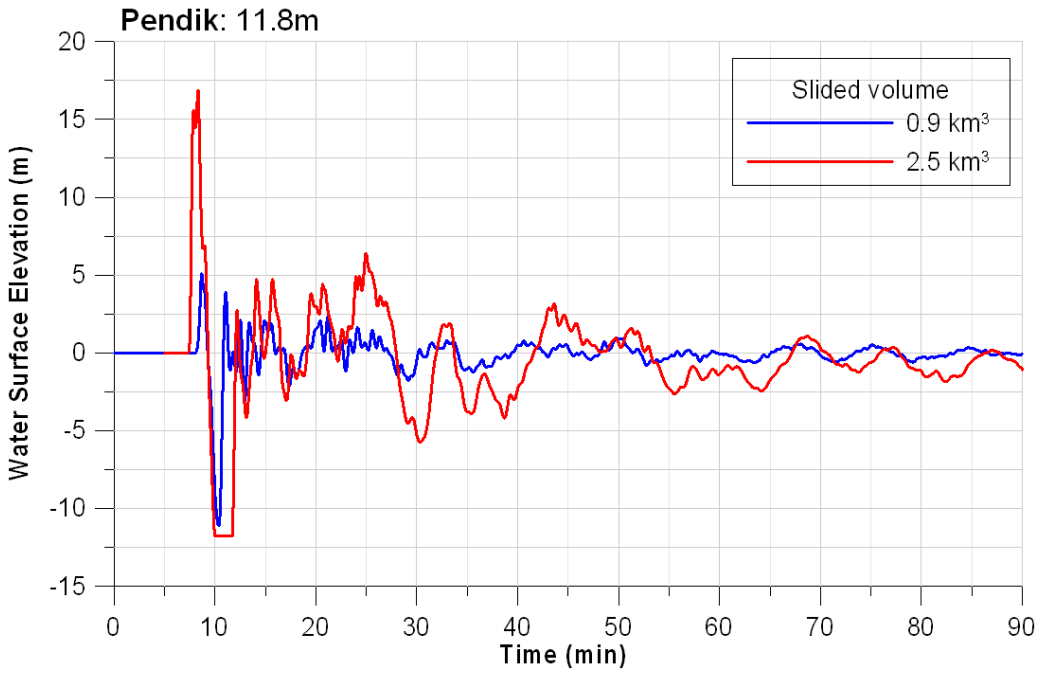

Figure 7.3: Comparison of water surface elevations for gauge point Pendik, for ON1 normal case (0.5 km^3 slide volume) and extreme case (2.5 km^3 slide volume)

To conclude, It must be pointed out that the submarine landslides may be responsible for generation of tsunamis and understanding more about the generation mechanisms of landslide triggered tsunamis is becoming more important for the mitigation strategies against tsunami hazards.

Tsunami science needs close cooperation between basic and applied sciences and also between international and local level authorities. The tsunami modeling and risk analysis are necessary for better preparedness and proper mitigation measures in the framework of international collaborations. Better understanding, wider awareness, proper preparedness and effective mitigation strategies for tsunamis need close international collaboration from different scientific and engineering disciplines with exchange and enhancement of existing data, development and utilization of available computational tools.

REFERENCES

Assier-Rzadkiewicz, S., Heinrich, P., Sabatier, P. C., Savoye, B., And Bourillet, J. F. (2000), *Numerical modelling of landslide-generated tsunami: The 1979 Nice Event*, Pure Appl. Geophys. 157, 1707–1727.

Bornhold, B.D., Thomson, R.E., Rabinovich, A.B., Kulikov, E.A.,Fine, I.V., 2001, *Risk of landslide-generated tsunamis for the coast of British Columbia and Alaska*, An Earth Odyssey 1450-1454

Fine, I.V., Rabinovich, A.B., Thomson, R.E., Kulikov, E.A., 2003, *Numerical modeling of tsunami generation by submarine and subaerial landslides*, Submarine Landslides and tsunamis 69-88

Fryer G.J., Watts P., Pratson L.F., 2004, *Source of the great tsunami of 1 April 1946: a landslide in the upper Aleutian forearc*, Marine Geology 203 201-218

Grilli, S.T., Watts, P., 2005, *Tsunami generation by submarine mass failure I: Modelling, experimental validation, and sensitivity analyses*, Journal of Waterway, Port, Coastal, and Ocean Engineering © ASCE November/December, 283-297.

Harbitz, C.B., Løvholt, F., Pedersen, G. & Masson, D.G., 2006, *Mechanisms of tsunami generation by submarine landslides: a short review*, Norwegian Journal of Geology Vol. 86, pp. 255-264

Hayir, A., Seseogullari, B., Kilinc, I., Erturk, A., Cigizoglu, H.K., Kabdasli, M.S., Yagci, O., Day, K., 2008, *Scenarios of tsunami amplitudes in the north eastern coast of Sea of Marmara generated by submarine mass failure*, Coastal Engineering 55, 333-356

Imamura, F., Imteaz, M.A., 1995, *Long waves in two layer, governing equations and numerical model*, Journal of Science Tsunami Hazards Vol.13 No.1, pp. 3-24.

Kilinc, I., 2008, *The effect of a possible submarine landslide to the coasts of Istanbul*, PhD Thesis (inTurkish), Istanbul Technical University, Institute of Natural Sciences,

Lee, H., Ryan, H., Kayen, R.E., Haeussler, P.J., Dartnell, P. & Hampton, M.A., 2006 *Varieties of submarine failure morphologies of seismically-induced landslides in Alaskan fjords*, Norwegian Journal of Geology, Vol. 86, pp. 221-230

Liu P.L.-F., Wu, T.-R., Raichlen, F., Synolakis, C.E., Borrero, J.C., 2005, *Runup and rundown generated by three-dimensional sliding masses*, J. Fluid Mech. Vol. 536, 107-144

Lopez-Venegas, A.M., ten Brink, U.S., Geist, E.L., 2008, *Submarine landslide as the source for the October 11, 1918 Mona Passage tsunami: Observations and modeling*, Marine Geology 254, 35-46.

Lynett, P., Liu, P.L.F., 2003, *Submarine landslide generated waves modeled using depth-integrated equations*, Submarine Landslides and Tsunamis, 51-58.

Masson, D.G., Harbitz, C.B., Wynn, R.B., Pedersen, G. & Løvholt, F., 2006, *Submarine landslides: processes, triggers and hazard prediction*, Phil. Trans. R. Society A 364, 2009-2039

Minoura, K., Imamura, F., Kuran, U., Nakamura, T., Papadopulos, G. A., Sugawara, D., Takahashi, T., Yalciner, A.C., 2005, *A tsunami generated by a possible submarine slide: evidence for slope failure triggered by the North Anatolian fault movement*, Natural Hazards 36: 297-306

Murty, T.S., 2003, *Tsunami wave height dependence on landslide volume*, Pure appl. Geophys. 160 2147-2153

Okal, E.A., Synolakis, C.E., 2003, *A theoretical comparison of tsunamis from dislocations and landslides*, Pure and Applied Geophysics 160, 2177-2188

Okal, E.A., Fryer, G.J., Borrero, J. C., Ruscher, C., 2002, *The landslide and local tsunami of 13 September 1999 on Fatu Hiva (Marquesas Islands; French Polynesia)*, Bull. Soc. Geol., France, t. 173, no 4, pp. 359-367

Okal, E.A., Synolakis, C.E., Uslu B., Kalligeris, N., Voukouvalas, E., 2009, *The 1956 earthquake and tsunami in Amorgos, Greece*, Geophys. J. Int. 178, 1533–1554

Ozbay, I., 2000, *Two layer numerical model for tsunami generation and propagation*, Ms. Thesis, Middle East Eechnical University, Department of Civil Engineering, Ocean Engineering Research Center, Ankara, Turkey

OYO and IMM, 2007, *Project report on simulation and vulnerability analysis of tsunamis affecting the İstanbul coasts*, prepared by OYO Int. co. (Japan) for Istanbul Metropolitan Municipality (IMM)
Simulation and vulnerability analysis of tsunamis affecting the Istanbul coasts, http://yalciner.ce.metu.edu.tr/marmara/index_eng.htm, last visited on August 2009

Pelinovsky, E., Poplavsky, A., 1996, *Simplified model of tsunami generation by submarine landslides*, Phys. Chem. Earth, Vol.21, No. 12, pp. 13-17.

Van Nieuwkoop, J.C.C., 2007, *Experimental and numerical modelling of tsunami waves generated by landslides*, Ms. Thesis, Delft University of Technology

Ward. S.N., Day, S., 2002, *Suboceanic landslides*, Yearbook of Science and Technology

Yalciner, A.C., Alpar, B., Altinok, Y., Ozbay, I., Imamura, F., 2002, *Tsunamis in the Sea of Marmara, Historical documents for the past, models for the future*, Marine Geology 190 445-463

Yalciner, A.C., Karakuş, H., Özer. C., Özturt, G., 2005, *Short courses on understanding the generation, propagation, near and far-field impacts of tsunamis and planning strategies to prepare for future events*, Course notes, METU Civil Eng. Dept. Ocean Eng. Res. Center